PHYSICAL REVIEW B

SOLID STATE

THIRD SERIES, VOL. 3, NO. 1 1 JANUARY 1971

Local Magnetic Fields in the Vanadium-Manganese Alloy System*

E. von Meerwall
Department of Metallurgy and Mining Engineering, University of Illinois, Urbana, Illinois 61801

and

D. S. Schreiber
Department of Physics, University of Illinois at Chicago Circle, Chicago, Illinois 60680
(Received 18 May 1970)

A study of the nuclear magnetic resonance (NMR) line shapes, Knight shifts, and linewidths of both ^{51}V and ^{55}Mn has been made between 1.4 and 300 °K in the vanadium-manganese alloy system, and is complemented by measurements of the magnetic susceptibility. The concentration dependence of the magnetic susceptibility shows a gradual decrease and is temperature independent to 30% Mn in V, followed by a temperature-dependent increase. Both V and Mn Knight shifts decrease rapidly above 40% Mn, but without most of the temperature dependence displayed by the susceptibility. Both shifts and susceptibility are analyzed in terms of the details of the $3d$-band structure in this and related alloy systems: A relatively flat $4s$ band is superimposed on two $3d$ subbands whose position is such that the Fermi level falls between their peaks in alloys at 45% Mn in V. In a more detailed consideration of the susceptibility, and both Knight shifts, it is necessary to depart from the rigid-band model by taking into account solute-solvent local electron density differences. The much smaller temperature dependence of the observed NMR parameters, when compared to that of the susceptibility above 45% Mn, is speculatively explained by the magnetization of Mn atoms determined by local Mn concentration, in reasonable agreement with the results. A Curie-Weiss component of the susceptibility above 40% Mn may have its origin in an itinerant magnetism based on the Anderson-Wolff band model as elaborated on by Schrieffer and co-workers. Strong field-dependent increases in the susceptibility below 85 °K are observed in alloys above 35% Mn, but the modest observed changes in the NMR parameters through this transition suggest that these magnetic phenomena originate in a small fraction of the sample volume. The effects of the nuclear quadrupole interaction, and of Knight-shift inhomogeneity, on the ^{51}V NMR are discussed in detail. The NMR in three σ-phase samples was observable for both nuclear species down to 1.4 °K, and the susceptibility is only moderately temperature dependent; no evidence of magnetic ordering was found.

I. INTRODUCTION

The first-row bcc transition-metal alloys have been studied in some detail in the past decade, especially since the advent of NMR and the Mössbauer effect as microscopic probes to complement the bulk measurements of specific heat and magnetic susceptibility (e.g., Refs. 1–21). The concentration dependence of their various properties has usually been described in terms of a rigid two-band model, [22–27] in which a flat $4s$ band is superimposed on two nonoverlapping $3d$ subbands, the lower having symmetry t_{2g} (antibonding), and the upper consisting of states having symmetries t_{2g} (bonding) as well as e_g. Recent band calculations[24] on V-Mn give densities of states in rough agreement with these concepts, as illustrated in Fig. 1.

According to the rigid-band model, comparisons among similar alloy systems may be made on the basis of an average electron-to-atom ratio $\mathfrak{z}$, calculated by counting electrons from the last closed shell. Some deviations from the rigid-band model are attributable to the effect of shielding the extra nuclear charge ΔZ and are roughly proportional in magnitude to ΔZ. These deviations are of two kinds: There are differences in electronic character between solvent and solute atoms, in general, as well as differences among members of each species. The latter arise mainly at higher solute concentrations as a result of the overlap of charge

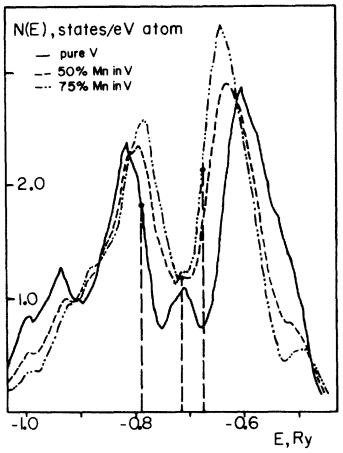

FIG. 1. Densities of state for three concentrations of disordered bcc V-Mn alloys, as calculated by Waber and Koskimaki (Ref. 24). Fermi levels are indicated by vertical lines.

clouds from the shielding of the excess solute nuclear charge, and are observable in microscopic measurements as local fluctuations in $\mathfrak{H}$ in response to random local solute concentration fluctuations. As will be shown, V-Mn ($\Delta Z = 2$) is in the intermediate region where there are sizable departures from the rigid-band model, but where a localized solute impurity state is not yet observable.

A number of NMR, susceptibility, and electronic specific-heat studies of V-based bcc transition-alloy systems have been performed.[1-21] The NMR study of V-Mn has the advantage of the observability of both solvent and solute NMR in highly abundant (both nearly 100%) nuclear species. The bcc concentration range has been extended from its equilibrium limit at[28] 51% Mn to near 70% by quenching. There also exists the ordered intermetallic compound VMn having the CsCl structure.[29,30]

In a comparison between V-Cr (paramagnetic at all temperatures below 95% Cr in V, i.e., 5.95 e/at., then antiferromagnetic at low temperatures) and V-Fe (ferromagnetic at low temperatures above 27% Fe, i.e., 5.86 e/at.), added interest is focused on the magnetic properties of the intermediate V-Mn system. The present investigation shows that while the system is essentially Pauli paramagnetic below 5.7 e/at., complex magnetic behavior occurs in bcc samples above 5.75 e/at. However, no bulk ferromagnetic or antiferromagnetic ordering is present below 6.5 e/at. Drain[13] reported observation of the ^{51}V NMR in a sample of 2% Mn in V, and Oda and Yamagata[31] that of the ^{55}Mn NMR in a 3% alloy. Their observations generally agree with ours, as presented in Sec. III. A preliminary report of the present investigation was given elsewhere.[32]

II. EXPERIMENTAL TECHNIQUES

Alloy samples for this study were prepared by arc melting, and in some cases also levitation melting. Starting vanadium was obtained from Materials Research Corp. (MARZ grade, 99.98% pure), or from Research Organic/Inorganic Chemical Co. (99.99% pure), and manganese from Johnson and Mathey (99.98% pure), some of which was subsequently vapor distilled. The achieved alloy concentration was determined on the basis of loss of Mn by evaporation. The uncertainty in the concentration determination is estimated to be ±1% Mn. About one-third of the samples were accorded heat treatment, following Waterstrat.[28] No difference was found in the Knight shifts, linewidths, susceptibilities, and x-ray lattice parameters between heat-treated and untreated sections of the same ingots.

Colorimetric analysis for trace nitrogen showed always less than 0.02% N, oxygen less than 0.1%, and transition-metal impurities for two specimens tested were less than 0.02%.[33] Microscopic examination of polished unetched bcc samples revealed small, dark pits in alloys above 30% Mn, concentrated near the grain boundaries and reaching their greatest extent near 57% Mn. At that concentration, the mean diameter of those discernible reaches 3×10^{-4} cm and their volume approaches 2% of the total sample volume. The use of vapor-deposited manganese somewhat reduced the size and incidence of these features.

The crystal structure of each specimen was checked by performing Debye-Scherrer x-ray diffraction on 200"-mesh powder of the alloys. In all cases below 70% Mn, the pure bcc structure was observed. Between 78 and 84% Mn, the observed identical complex spectra are ascribed to the σ phase. One sample at 76% Mn displayed a spectrum consisting of both bcc and σ reflections. The bcc spectra were measured and lattice parameters a_0 were calculated using a computer program. The concentration dependence of a_0 is shown in Fig. 2; the linear decrease of a_0 from 3.028 Å

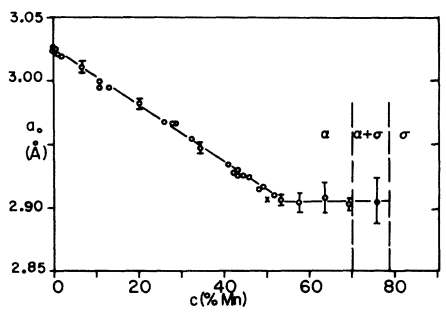

FIG. 2. X-ray bcc lattice parameters versus Mn content in V-Mn at room temperature. Definition of symbols: open circles, bcc present only; closed circle, bcc in mixed (with σ phase) system; cross, bcc CsCl ordered.

at pure V proceeds to 2.903 ± 0.003 Å at 52% Mn [the equilibrium $\alpha/(\alpha+\sigma)$ phase boundary]. No line broadening due to stress or composition inhomogeneity was observed.

To obtain powders for the NMR work, samples below 25% Mn had to be filed, whereas crushing and grinding was used at higher concentrations. All filed powder was magnetically "sieved" using a small permanent magnet. All powders were passed through a 325-mesh sieve; the resulting maximum particle size is a fraction of the classical rf skin depth at 300 °K and 12 MHz for both V and Mn metal.

A conventional cw NMR spectrometer employing a Pound-Knight marginal oscillator and phase-sensitive detector was used with a Varian 12-in. field-regulated electromagnet. When encountering small signal-to-noise ratios, especially in the Mn spectra and generally above 35% Mn, the necessary signal enhancing was performed using a Nuclear Data Enhancetron model 1024. The NMR experiments were performed at temperatures between 1.4 and 300 °K in a conventional liquid-helium cryostat.

The magnetic susceptibility of a series of bulk specimens was measured between 77 and 400 °K at 1.5 and 2.5 kOe with an electrobalance and a small electromagnet equipped with constant-force pole pieces. The field dependence (1–14 kOe) between 1.8 and 90 °K was checked in a separate experiment for several samples above 11% Mn.

III. RESULTS AND DISCUSSION

The expected quadrupolar distortion of the ^{51}V spectra in the alloys is clearly observable, but remarkably small. A full discussion of these effects is given in Appendix A. For the purpose of separating these from the other results, their main features will be summarized here: (a) The quadrupole distortion is of only first order for fields above 4 kOe. No field or temperature dependence of the line shape can be attributed to it. No further distortion is observed above 15% Mn, where about 0.8 of the peak-to-peak intensity resides in a region somewhat outside the central peak. (b) The peak-to-peak width at all concentrations is unaffected by this distortion, as is the position of the absorption maximum. The entire expected intensity per V nucleus can be recovered from an integration of the visible NMR absorption over a 250-KHz region. Thus, it may be seen that the results of Knight-shift and linewidth experiments can be interpreted largely without reference to quadrupolar effects.

A. NMR Knight Shifts and Linewidths

A study of the Knight shifts K and the linewidths ΔH for both the ^{51}V and ^{55}Mn NMR was performed at several temperatures and fields for all samples in the bcc region, including two samples having partially CsCl structure. Above 40% Mn, ΔH was found to be due mainly to microscopic Knight-shift inhomogeneities. This is discussed in detail in Appendix B. Three samples having σ-MnV structure were similarly examined.

Knight shifts are quoted as field shifts, and, in the case of ^{51}V, were measured with respect to $NaVO_3$ or secondary standards such as ^{63}Cu, ^{51}V, and ^{27}Al in the pure metals. All V alloy shifts shown represent averages of between 6 and 15 separate determinations.

Because of the difficulty[34] in defining a meaningful primary standard for a chemically unshifted ^{55}Mn resonance, the secondary standards described above were used to calibrate the Mn shifts as well. All shifts were measured to the zero-signal intercepts in the differential spectra. The distinction between the measured modal shift (most probable) and the mean shift becomes important in the asymmetric spectra above 40% Mn, where it causes some overestimation of both V and Mn mean shifts.

The linewidths at all concentrations are reported as differences in field between extrema in the differential spectrum recorded at constant frequency. This measure was found to be independent of quadrupolar distortion, and remains useful in the presence of asymmetry in both spectra since the latter was always accompanied by a broadening of all features of the resonance. All values of linewidth shown represent averages over at least four measurements for the sample at the given temperature and field.

1. *Results*

The results of the study of the room-temperature concentration dependence of the Knight shifts are shown in Figs. 3 and 4. These measurements were

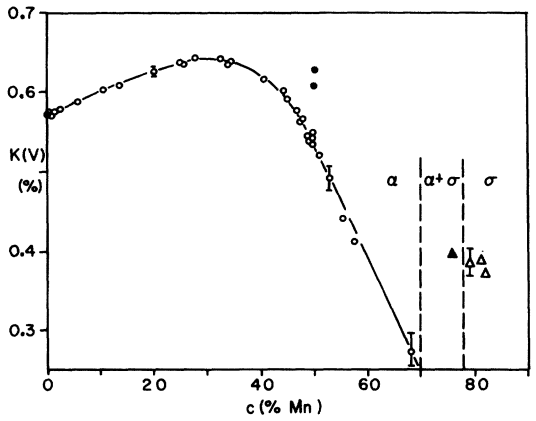

FIG. 3. Room-temperature ^{51}V Knight shifts in V-Mn, as a function of Mn content. Symbols: open circles, bcc random; closed circles, bcc CsCl ordered; open and closed triangles with vertex up, in pure and mixed σ phase.

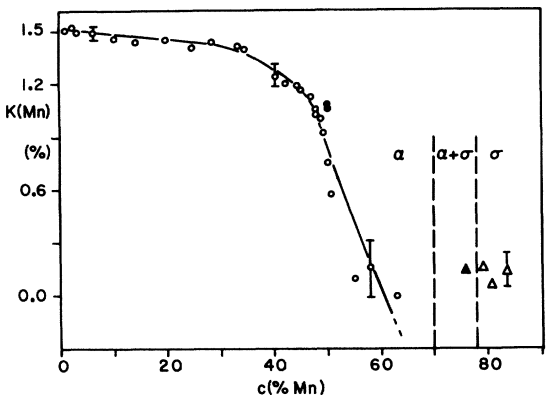

FIG. 4. ^{55}Mn Knight shifts in V-Mn as function of manganese concentration at room temperature. Symbols as in Fig. 3.

performed between 11.4 and 12.6 kOe, but extensive checks between 5.6 and 16.7 kOe failed to reveal any field dependence in any sample. The vanadium Knight shift rises from 0.570% at pure V to a broad maximum of 0.645% near 30% Mn. Thereafter, the shift decreases to below 0.3% above 65% Mn in V. [In a bcc sample of 76% Mn in V recently supplied to us by P. A. Beck, and H. Claus, K(V) was found to be K(V) = 0.15% at 300 °K and 0.13% at 77 °K.] The presence of line broadening and asymmetry in the high-concentration region are attributable to microscopic spatial inhomogeneties in the Knight shift. The observed shifts and peak-to-peak linewidths in two partially-CsCl-ordered intermetallic samples may be attributed directly to the CsCl structure because of the strong emphasis in the differential spectrum on narrow features, characteristic of the structurally ordered phase. The shift of the broad but symmetric σ-phase vanadium spectrum is (0.380 ± 0.005)%.

The temperature variation of the vanadium Knight shift was invariably found to be small below 40% Mn in V. In this region, the shift change $\Delta K = K(300\ ^\circ\text{K}) - K(1.5\ ^\circ\text{K})$ was always less than +0.02%. An increase in the shift-temperature dependence was observed above 40% Mn. The results for a *random* alloy of 50% Mn in V are displayed in Fig. 5.

A small discontinuity is observed in both shifts near 80 °K. Corresponding effects are observed in both NMR linewidths (Sec. III A 3) and the magnetic susceptibility (Sec. III B). The strength of these effects has a correlation with the occurrence of the holes, or inclusions, visible in the metallographic study. In the four most strongly affected samples, between 50 and 60% Mn, an additional narrow ($\Delta H \approx 15$ Oe) line was observed in the ^{51}V spectrum with a shift of (0.650 ± 0.006)%. At room temperature, this line had a relative intensity of the same magnitude as the fractional volume of the dark features observed metallographically, not exceeding 2.5%. This line decreased in intensity below 100 °K and was unobservable below 60 °K. Simultaneously, the visible NMR of both V and Mn is broadened and reduced in intensity. While the broadening effect is largest near 55% Mn, the intensity reduction is greatest at the highest bcc concentrations, reducing the V intensity by about 80% near 70% Mn. The deformation of the NMR lines, the presence and temperature-dependent intensity of an extra line, and the effects on magnetization and susceptibility are strongly suggestive of the presence of finely dispersed aggregations of a ferromagnetic metallic compound associated with the visible inclusions. Another explanation for these and similar phenomena in V-Mn has been proposed[35] involving the occurrence of a complex magnetic phase transition in bcc V-Mn near 90 °K, characterized by the formation of separated magnetic clusters in manganese-rich environments. It is quite possible that there is some kind of ferro- or ferrimagnetic aggregation which forms in the high-concentration Mn samples. Whether they are associated with statistically occurring Mn-rich regions or with imperfections is not clear. It is apparent, however, that since the V and Mn resonances still persist at low temperatures and high Mn concentrations, only a small fraction of the sample can be magnetically ordered.

In Fig. 4 the shifts of the ^{55}Mn NMR are shown versus manganese content. After an initial gradual decrease from 1.50% in the dilute regime to 1.38% near 34% Mn, there follows a more rapid decrease toward zero shift near 65% Mn, accompanied by extreme asymmetry and broadening, which is, again, attributable to the sensitivity of K to the microenvironment, as evidenced by the characteristic field dependence of the linewidths. The temperature dependence of the manganese shifts above 40% Mn is only slightly more pronounced than that of K(V), but is more difficult to measure because of the much larger widths. The absence

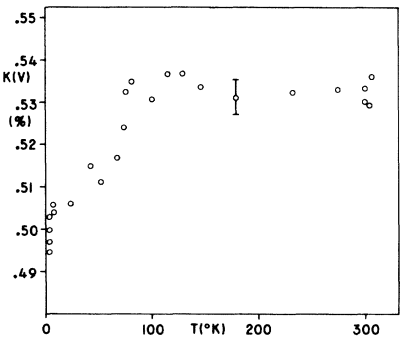

FIG. 5. Vanadium Knight Shift versus temperature in a disordered alloy of 50% Mn in V, between 10 and 12.5 kOe.

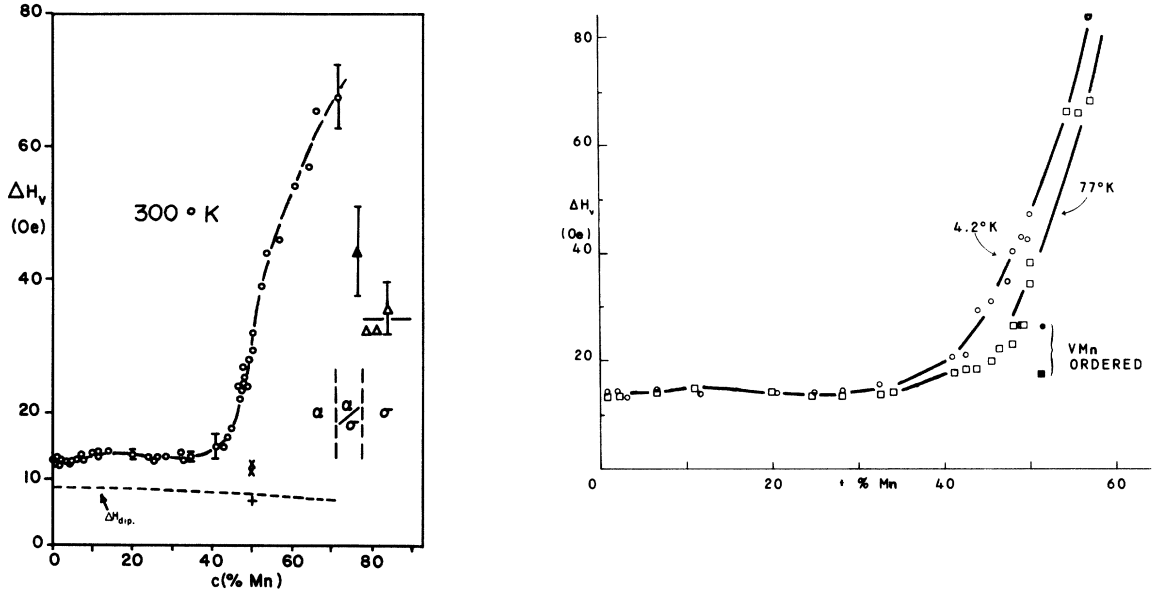

FIG. 6. ^{51}V NMR linewidths in V-Mn as function of Mn content at 11.9 kOe, 4.2, 77 °K on (b) and 300 °K on (a). Crosses denote samples having CsCl order. The calculated dipolar width is indicated by a dashed line and by a plus for the CsCl structure.

of a more pronounced temperature dependence of the Knight shifts, and the absence of an H/T broadening of the resonances (Sec. III A 3) below 65% Mn, is an indication that any localized magnetic moments present have little effect on the observed NMR spectra and may be entirely confined to the most Mn-rich regions. The small NMR intensity arising from such regions will be broadened and shifted out of the region of observation.

In a similar manner to the V shift, the Mn shift in the ordered intermetallic alloys is slightly larger than for equivalent disordered alloys. Because of the expected sensitivity of the shift to the microenvironment, it is evident that the details of that dependence differ between K(V) and K(Mn); while K(Mn) seems to reflect the locally decreased Mn concentration in the CsCl structure by the resemblance to shifts in disordered alloys containing less than 50% Mn, this simple picture is not appropriate for K(V). The manganese shift in the σ phase is $(0.12 \pm 0.05)\%$.

The concentration dependence of the vanadium

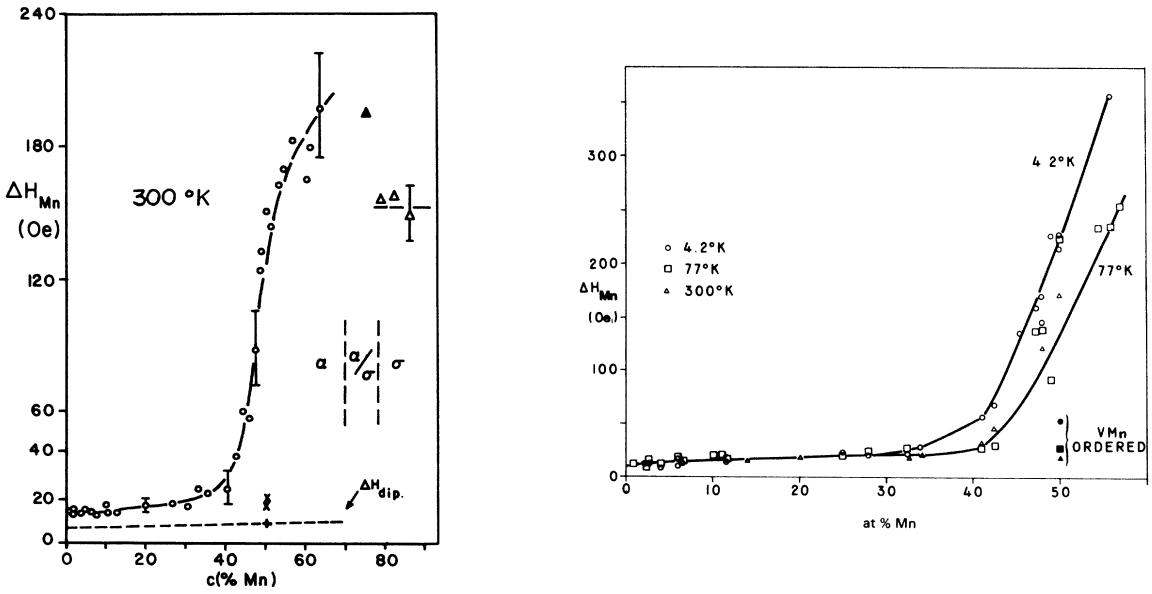

FIG. 7. ^{55}Mn NMR linewidths-versus-Mn content, at 11.9 kOe, 4.2, 77 °K on (b) and 300 °K on (a).

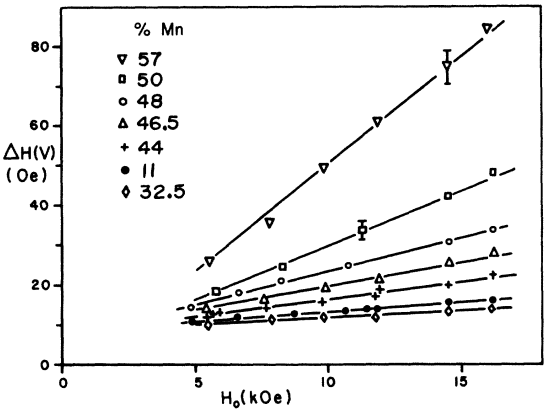

FIG. 8. Field dependence of the vanadium linewidths in V-Mn at 300 °K. Symbols denoting % Mn: triangle, vertex down, 57%; square, 50%; open circle, 48%; triangle, vertex up, 46.5%; plus, 44%; closed circle, 11%; diamond, 32%.

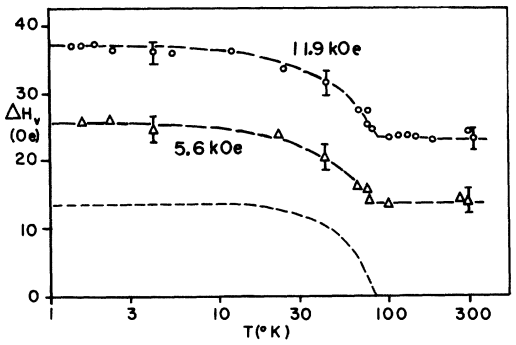

FIG. 9. ^{51}V NMR linewidths versus temperature at two values of field, open circle 11.9 kOe and triangle 5.6 kOe, in a sample of 48% Mn in V. The width increase below 100 °K reflects the emergence of nonuniform magnetization. The log scale for T is used merely to conveniently display all the data. The line without symbols is a superimposed magnetization curve in the molecular field approximation for $J=2$.

and manganese linewidth at 11.9 kOe and various temperatures are shown in Figs. 6 and 7. The calculated nuclear dipolar linewidths are also shown as function of concentration and for the CsCl structure. In these calculations, Van Vleck's second moment formula[36] was used with the measured x-ray lattice parameters, under the assumption of a Gaussian line shape. For both resonances, the observed linewidths remain small until above 35% Mn, where their increase correlates with the rapid changes in the corresponding Knight shifts. Figure 8 shows the room-temperature V linewidths of selected samples as a function of applied field. Significant field dependence first emerges above 35% Mn. The temperature dependence of the width in a 48% alloy at two values of field is shown in Fig. 9, and suggests by its more pronounced field dependence that most of the line broadening at this concentration is attributable to Knight-shift inhomogeneity. The change in width below 100 °K is observed in all samples above 35% Mn and is most pronounced near 57%. It is accompanied by a change in the line shape, especially in the spectral wings (see Fig. 10). The amount of this distortion and the temperature of its onset coincide with that of the field dependence of the susceptibility and the presence of hysteresis effects in the magnetization in the same ingots. The distortion of the NMR spectra is characteristic of the effects of finely dispersed aggregations of magnetized matter on the NMR of the nonmagnetic bulk of the sample. In the presence of these effects, a broadening due to possible magnetic moments in the upper 3*d* subband forming uniformly in the alloys was obscured. After approximate corrections were made for this temperature dependence and the field dependence from Knight-shift inhomogeneity, no broadening could be ascribed to uniformly distributed magnetic moments, even at the highest bcc concentrations. No loss of ^{51}V absorption intensity per V nucleus is observed in any sample above 100 °K. Since the quadrupolar distortion is small and, in any case, complete above 15% Mn, the line shape at all higher concentrations above 100 °K is due equally to all V^{51} nuclei in the alloy. Some intensity loss is evident in the ^{55}Mn spectra at all concentrations and temperatures, probably as the result of a larger quadrupolar distortion. Unless specified otherwise, values of Knight shift and linewidth referred to will be those at 300 °K.

2. *Comparison of* ^{51}V *Knight Shifts with Other V-Based Alloy Systems*

The over-all features of the concentration dependence of the V shift are repeated, with significant differences, for many V-based alloy systems. In particular, the peak in K(V) near 5.6 e/at. occurs in most V-transition alloy systems. However, the initial rise with addition of an equal total

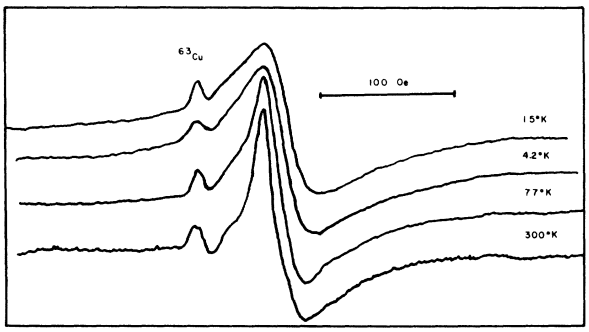

FIG. 10. ^{51}V NMR in a sample of 51% Mn in V at 11.9 kOe. The distortion in the wings of the spectra at low temperatures is characteristic of the presence of discrete aggregations of magnetization.

number of electrons from solute atoms is observed to vary among alloy systems. A comparison of the results of the present work with other investigations shows a markedly systematic variation in the slope of K(V) versus average alloy electron concentration near pure V, if that quantity is plotted as function of the electron concentration of the pure solute (Fig. 11). A similar observation applies to the peak of the shift relative to the shift in pure V metal. The interstitial vanadium hydride is included in this comparison with the assumption[19] that the hydrogen's electrons enter the alloy conduction bands.

From an inspection of Fig. 11, it may be observed that while the main response of K(V) is to the average electron density, it also reflects the differences in charge distribution resulting from the presence of solvents with differing nuclear charges. The systematic departure from a rigid-band scheme, evident in Fig. 11, may be interpreted in terms of an increasingly tight screening of the increasing extra nuclear charge ΔZ.[37] From the negative slope and the approximate linearity of the relation in Fig. 11, it appears that the response of the electron system to the extra nuclear charge is not strictly additive, but that a linearly increasing fraction of each extra electron is used for screening positive, increasing solute nuclear charges. By comparing the value of $(\Delta K/\Delta \vartheta)_5$ extrapolated to V in V metal with the measured value for Mn in V, it may be inferred that of the two extra electrons which Mn brings to the alloy V-Mn, only about 75% or more contributes to the V-shift increase, the remainder presumably adding an excess local occupancy of $\Delta\rho \lesssim 0.55\ e$/at. to the 3$d$ band near Mn atoms. A simple model is proposed to illustrate this estimate of $\Delta\rho$ and is developed in Appendix C.

Since an analysis of the vanadium line shape (Appendix B) shows that the Knight shift senses the occupancy of mainly the first two neighbor shells, this range must represent the mean electronic screening radius; a similar conclusion was reached for V-Cr.[14] Thus, it is necessary that each of the 14 atoms surrounding a Mn atom carry the remaining shielding charge of about 0.1 electron each for the screening to be complete. However, at increasing ΔZ, as in V-Co or V-Ni, it may be inferred from Fig. 11 that screening begins to take place mainly in the 3d shell of the solute atom, as is qualitatively expected in a more local impurity situation with higher ΔZ. V-Mn seems to be in an area where the rigid-band model is no longer very helpful, but where a local description is not yet appropriate. The latter point is emphasized by the notable absence of broadening and shift ascribable to charge-density oscillations arising from conduction-electron scattering from charge impurities. Thus, the work of Langer and Vosko,[38] and Kohn and Vosko[39] as applied to NMR results[40] is clearly not appropriate to this case (see also Appendix A). The most appropriate explanation of the increases in V shift with addition of Mn, Cr,[14,19] and Fe[7] is the increasing electronic occupancy of the lower 3d subband (see Fig. 1), whose decreasing density of states at the Fermi surface causes a decrease in the negative core-polarization contribution to K [see Sec. IV, Eq. (6)]. This effect is reproduced in a partitioning of shift and susceptibility presented in Sec. IV.

It may be argued that part of the decrease in the initial slope of K(V) versus ϑ with increasing ΔZ originates in the decrease in atomic solute concentration needed to produce the given ϑ, say, 5.1 e/at.; fewer V atoms will have a shift characteristic of impurity proximity for solutes with high ΔZ than for those with low ΔZ. While this effect would indeed cause a lower rate of increase of the model shift at higher ΔZ, the attendant greater linewidth and possible asymmetry have not been observed at the appropriate low concentrations. Contrary to the case of the silver-based alloys,[40] no useful upper limits can be placed on this effect in vanadium alloys because of the relatively large V linewidth coupled with the small rates of shift increase and the distortion caused by quadrupolar broadening. For purposes of Knight-shift interpretation at low-transition impurity concentration in V, any electrons not used to screen excess nuclear charge by remaining associated with the impurity site are distributed in the wider impurity vicinity so as to simulate a more or less uniform electron density near V atoms. This analysis ceases to be valid at higher-impurity concentrations in V-Mn, where the overlap of the charge clouds causes local variations in K(V).

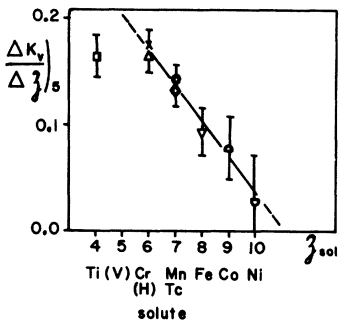

FIG. 11. Ratio of Knight-shift change to e/at. change in the solid solution near 5.0 e/at. in V-based alloys as function of the solute e/at. ratio ϑ: V-Ti (Ref. 9)(square); VH_X (Refs. 19 and 20) (cross); V-Cr (Refs. 9 and 14) (triangle, vertex up); V-Mn (present work) (circle); V-Tc (Refs. 9 and 15) (diamond); V-Fe (Ref. 7)(triangle, vertex down); V-Co (Ref. 13)(semicircle, convex up); and V-Ni (Ref. 13)(semicircle, convex down).

The local electronic charge density differences between V and Mn may be described crudely in the band picture, using the known details of the subband structure of the first transition alloys (see also Fig. 1). The density of states near Mn, while probably of shape similar to that near V, will be displaced to lower energies, so that the Fermi level will fall much nearer the higher end of the lower $3d$ subband, corresponding to an electron concentration near or below 5.5 e/at. This hypothesis is illustrated schematically in Fig. 12. It is expected that the upper $3d$ subband will begin to be occupied first near Mn atoms, and that properties such as the temperature dependence of the susceptibility will originate with Mn atoms. Some differences in the concentration dependences of K(V) and K(Mn) may be qualitatively understood on this basis (see Sec. IV). Other differences may be due to those in the Coulomb interactions in V and Mn. These will be ignored here because of their complexity; it is plausible that the differences in Coulomb interaction would tend to emphasize a more local magnetic character of Mn in V. It should be emphasized that for this and other reasons the similar-but-displaced band picture used here[25] has only semiquantitative validity in this complicated alloy system. Its extensive use in Secs. III B and IV should be regarded with these limitations in mind.

3. *Linewidths*

The nuclear dipolar contribution to the linewidth accounts for the largest fraction of both V and Mn widths up to 45% Mn. The small decrease with concentration of the dipolar contribution to the vanadium linewidth accounts for the apparent decrease in widths between the 11% sample and the 32.5% sample in Fig. 8. A further, smaller contribution to the widths is a broadening by macroscopic magnetic field inhomogeneties from varying demagnetizing fields in the metal particles.[41] This is the source of the small field dependence of the linewidth even in pure V. Drain's numerical calculations of the line shape in V metal show that this effect adds 1–2 Oe to the linewidth at 12 kOe.[41] These contributions nearly account for the V linewidths near pure V and near 30% Mn in V. The small remainder is attributed to pseudodipolar and indirect exchange broadening. Between 10 and 25% Mn, and, much more strongly, above 35% Mn, an additional contribution arising from local Knight-shift variation, is added to the field dependence of the widths. This effect is analyzed in detail in Appendix B.

Except for the broadening due to the presence of the discrete aggregations of magnetized matter in V-Mn above 45% Mn, the absence of an H/T broadening attributable to magnetic moments is similar

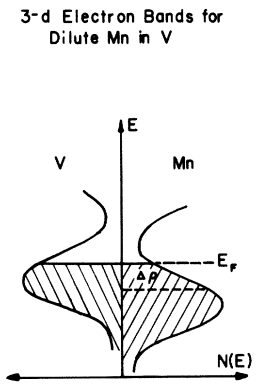

FIG. 12. Schematic illustration of the solute- and solvent-band occupancy for dilute Mn in V. The occupation of the Mn band exceeds that of the V band by $\Delta\rho$.

to the case of V-Fe.[7] There, the onset of Curie-Weiss behavior in the observed susceptibility near 21% Fe in V is not followed by temperature-dependent line broadening until 27% Fe in V, where ferromagnetism first appears at the lowest temperatures.

A similar analysis is appropriate in the case of the ^{55}Mn resonance. The linewidth in the dilute regime exceeds the simple dipolar and demagnetization widths by about 5 Oe, for which a non-Gaussian line shape and pseudodipolar indirect exchange, and possibly second-order quadrupolar broadening, may be responsible. Since the nuclear quadrupole moment of ^{55}Mn is about three times that of ^{51}V, second-order broadening may be expected at low fields, and first-order wipeout is expected to be complete well below 10% Mn. The first-order satellites are probably well removed from the central transition, consistent with the fact that the integrated intensity of the visible Mn spectrum per Mn nucleus is regularly found to be only upward of one-half that of the V resonance per V nucleus in the same sample.

In the Mn spectrum, no distortion or loss of intensity were attributable to second-order quadrupolar effects above 10 kOe, due to the absence of broadening proportional to inverse applied field. Low-field studies of the Mn line shape were made nearly impossible by the proximity of the relatively much stronger vanadium spectrum.

The resonances in the σ-phase samples were nearly symmetric and had broad wings. Their large widths and field-dependent broadening most likely arise from the presence of large first-order quadrupolar interactions and the presence of several different sites having characteristic Knight shifts. Since both spectra were observable and unaffected in width or strength down to 1.5 °K, the absence of bulk ferromagnetic or antiferromagnetic order must be inferred.

B. Magnetic Susceptibility

1. *Results*

The magnetic susceptibility at 1.5 and 2.5 kOe was measured for 18 bulk samples as a function of temperature between 77 and 400 °K. In several samples, measurements were also made of the magnetization and the field dependence of the susceptibility up to 14 kOe, down to 2 °K. The values of χ at 130 and 300 °K are displayed as functions of Mn concentration in Fig. 13. The initial decrease from pure V to 45% Mn is followed by a temperature-dependent increase, which continues to the end of the effective bcc solid solubility. This concentration dependence is in agreement with other recent work.[35] The temperature dependence in several samples is displayed in Fig. 15. Only a very small temperature dependence was found in samples below 35% Mn; two samples of σ-phase constitution also showed no pronounced temperature dependence.

Whereas no field dependence in χ was detected at any temperature for samples below 30% Mn, and above 90 °K for any sample, a pronounced field dependence of the as-measured χ occurred below 90 °K in bcc samples between 32 and 68% Mn. For samples in this region, when field cooled through the temperature range near 90 °K, the field-dependent susceptibility follows a relationship of the form

$$\chi(H) = \chi_\infty(H \to \infty) + M(T)/H \ , \qquad (1)$$

where $M(T)$ generally resembles the magnetization of a ferromagnetic material with a Curie temperature near 85 °K. The value of $M(T \to 0)$ and the strength of hysteresis effects in the low-temperature magnetization are largest near 57% Mn and correlate in magnitude with the previously described NMR line-shape distortion.

Similar effects have recently been observed[35] in the low-temperature specific heat in addition to the magnetic susceptibility, and have been attributed to a complex magnetic phase transition. However, the possibility of contamination by discrete clusters of a ferro- or ferrimagnetic Mn-containing aggregation ($T_{Curie} \approx 85$ °K) cannot be excluded in a consideration of the present data. Analyses[33] show a total impurity level of 0.07% or less even in the most strongly affected samples, while the visibly imperfect region in the sample approaches 2.5%. It is conceivable that magnetic Mn or V-Mn regions may be associated with, or may form near, these or other impurities or imperfections in the alloy during solidification.

By making low-temperature susceptibility measurements as a function of applied field and extrapolating to infinite field, as shown in Fig. 14, we are able to extract the correct intrinsic value of χ at low temperatures.[42] We estimate that the moment in the ferromagnetic aggregation is nearly

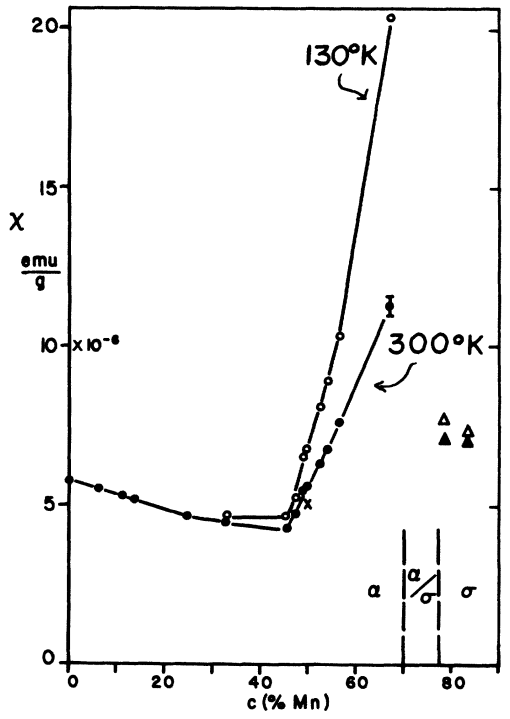

FIG. 13. Magnetic susceptibility in disordered V-Mn alloys versus Mn content. Open symbols are for 130 °K, solid symbols are for 300 °K; circles, bcc; triangles, σ phase; cross, CsCl ordered.

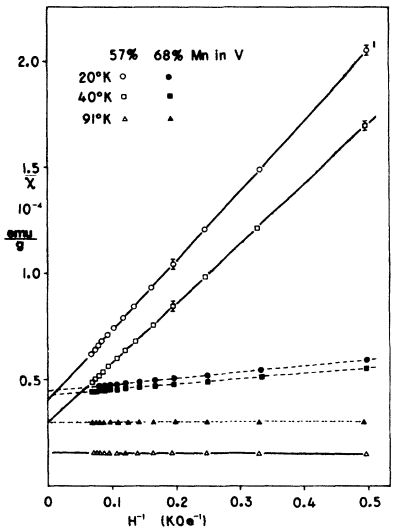

FIG. 14. Dependence of susceptibility on inverse field in two high-concentration samples. If the field dependence below 85 °K is interpreted in terms of ferromagnetic inclusions, then the infinite-field extrapolations represent the desired intrinsic alloy susceptibility. The largest field dependences were observed in samples near 57% Mn in V. To eliminate some hysteresis effects, H was cycled to +15 kOe before each set of measurements.

saturated at 20 °K and below. If one assumes, for example, that there is $2\mu_B$ per Mn atom in the aggregation, then from our infinite-field extrapolation data, we find that $M_0(H \to \infty, T \to 0) \cong 0.35$ emu/g, i.e., only about 0.1% of the total sample is to be associated with the ordered magnetic phase for the 57%-Mn sample. For the 68%-Mn sample, $M_0 = 0.03$ emu/g, or only ~ 0.01% of the sample is magnetically ordered.

If the effective moment associated with those Mn in the aggregations is smaller than $2\mu_B$, then the amount of sample participating in the magnetic phase is correspondingly greater. Even if the moment were as small as $0.02\mu_B$ per Mn, the maximum amount of sample bound up in the ferromagnetic aggregations would still be only 10%. That a fair fraction of the sample does not so magnetically order is evidenced by the persistence below 90 °K of at least part of both the V^{51} and Mn^{55} resonance intensity at high-Mn concentrations. Within the ordered aggregation and in the near vicinity, the large local fields present would remove the V^{51} and Mn^{55} resonances from observability. It seems reasonable to infer from our various observations that on the order of at most a few percent of the Mn in the sample is bound up in what might be called a ferro- or ferrimagnetic contaminate below 90 °K.

The complex magnetic behavior is not attributable to the σ phase; the described effects were weakly present in only one σ-phase sample, which contained 4% bcc structure.

In Fig. 15, all susceptibility values represent $\chi(H \to \infty)$; values below 90 °K represent extrapolations to infinite field. The changes of slope in χ^{-1} versus T occurring near 100 °K (for the 68% sample) to near 150 °K (for the 45% sample) are not to be associated with the dispersed ferromagnetic aggregations, whose contribution to χ is presumably eliminated in an infinite-field extrapolation, which was never, for any case, necessary above 90 °K. The temperature dependence of χ above 45% Mn in V, above 100 °K, is increasingly typical of a Curie-Weiss–like behavior, particularly at the highest Mn concentration. If one chooses to describe this behavior in terms of classical localized magnetic moments, associated with the Mn atoms, the effective magnetic moment per Mn atom rises to $1.56\mu_B$ at 68% Mn. It may be speculated that magnetic ordering of the bcc phase may set in above 80% Mn; similar behavior is observed in V-Fe, where ferromagnetic ordering above 28% Fe in V follows an approach to Curie-Weiss behavior.

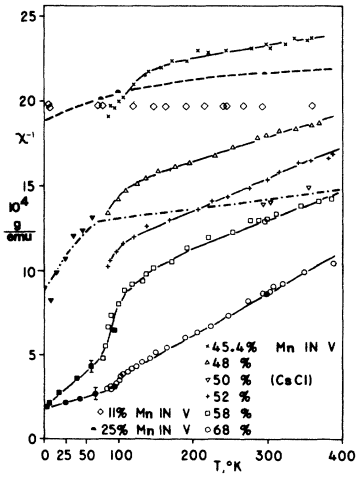

FIG. 15. Temperature dependence of the reciprocal magnetic susceptibility in bcc V-Mn. Solid symbols denote high-field extrapolation values. The triangle, vertex-down points are the data of D. Lam (private communication) on a mostly CsCl-ordered 50% sample.

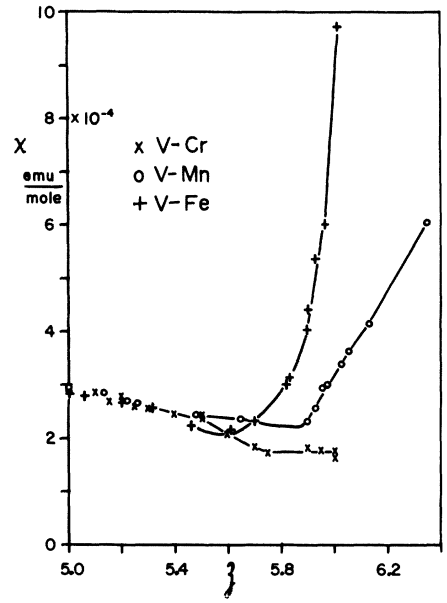

FIG. 16. Room-temperature magnetic susceptibility versus electron concentration $\mathfrak{z}$ in V-based alloys showing the effects of solute-solvent charge difference. Data for V-Cr (crosses) are taken from Refs. 2 and 4 and for V-Fe (plus signs) from Ref. 7. Circles are V-Mn. Four values for V-Mn below 5.1 e/at., given in Ref. 2, agree with the concentration dependence shown here.

2. *Discussion*

The general features of the concentration dependence of the susceptibility up to 5.6 e/at. may be compared with those of other V-based alloy systems. Close agreement exists between V-Cr, [2,4] V-Mn, [2] V-Tc, [2] V-Fe, [2,7] and also V-Co and V-Ni. [2] The differences in behavior above 5.6 e/at. begin to reflect differences between occupancy of orbitals in the upper 3d subband. Figure 16 displays room-temperature susceptibility values for V-Cr, V-Mn, and V-Fe versus average electron concentration. It is apparent that effects associated with the upper

$3d$ subband occur earliest in cases for which the solute-solvent charge difference ΔZ is highest, consistent with an increased localization of electronic charge near the higher-Z solute cores. In order to estimate crudely an effective solvent-solute charge difference $\Delta\rho$, a definition of the average e/at. ratio $\bar{e}$ will be used to relate local and average electron densities. It is desired to solve this equation for that local vanadium electron density e'_V, at that solute concentration c' at which occupancy of the upper $3d$ subband first occurs near solute atoms. Various authors have identified the onset of occupation of the upper $3d$ subband with the point where the electronic specific-heat coefficient begins to rise, or at above 5.6 e/at.[4,6,21] In these cases, a parallel increase of χ (often accompanied by an emerging Curie-Weiss temperature dependence) occurs at the same point. This has been confirmed for V-Mn by recent measurements.[35] Using the previously suggested model employing a common band structure near solute and solvent atoms with an appropriate solute-dependent shift to lower energies near solute atoms,[25] the solute electron concentration at the bottom of the upper $3d$ subband, e'_s, is identical for different alloy systems. It may be most closely estimated from data in systems with smallest ΔZ and hence, smallest $\Delta\rho$. The obvious candidate V-Cr shows small increases in electronic specific heat and susceptibility, as well as an emerging antiferromagnetism just below 6.0 e/at. Since $\Delta\rho$ is probably finite even in V-Cr, our best estimate will be $e'_s \gtrsim 6.0$ e/at.,

$$\bar{e} = (1-c')e'_V + c'e'_s, \quad e'_s \gtrsim 6.0\ e/\text{at.}, \qquad \Delta\rho \equiv e'_s - e'_V . \tag{2}$$

From an inspection of Fig. 16, the values of $\bar{e}'$ and c' at the onset of temperature-dependent increases may be used to derive estimates for $\Delta\rho$. The appropriate parameters are collected in Table I for V-Cr, V-Mn, and V-Fe. Because e'_s is a lower limit, the values of $\Delta\rho$ will also be lower limits. The value of $\Delta\rho$ found for small concentrations of Mn using Knight-shift results (see Sec. III A 2 and Appendix C) is larger. This may, in fact, be a real variation of $\Delta\rho$ with concentration.[43] However, since both estimates of $\Delta\rho$ are crude and since the model employed using $\Delta\rho$ is admittedly a gross approximation, it should suffice to use only a single average value of $\Delta\rho_{V\text{-}Mn} = 0.3 \pm 0.1$ e/at. Also, the unknown differences in the Coulomb interaction in different alloy systems are another source which make this estimate only semiquantitatively reliable. In view of the systematic variation between alloy systems of the Knight shift at all electron concentration, the close agreement between susceptibility values below 5.6 e/at. may

TABLE I. Solvent-solute electron density differences from susceptibility results.

Alloy system	$\bar{e}$ (e/at.)	c'	$\Delta\rho$ (e/at.)
V-Cr	(6.0)	(1.0)	($\gtrsim 0.0$)
V-Mn	5.9	0.45	$\gtrsim 0.2$
V-Fe	5.7	0.24	$\gtrsim 0.4$

at first appear fortuitous. A brief analysis will reveal the reason for this agreement. If the $3d$-state density at the Fermi surfact arises only from the lower $3d$ subband (as is the case below 5.6 e/at. certainly up to V-Fe), then the effect of the presence of a $\Delta\rho$ will be a proportional shifting of the bands relative to the Fermi level (see Sec. III A 2). If, as is probably the case, the lower $3d$-band Fermi-state density decreases almost linearly with electron density above 5.0 e/at. the concentration-sensitive parts of the susceptibility (see Sec. IV) will at first decrease linearly for both types of sites, irrespective of the magnitude of $\Delta\rho$. This state of affairs is indistinguishable from a dependence purely on average electron concentration, until upper $3d$-subband character appears near solute atoms. Thus, the observance of agreement of susceptibility (and electronic specific heat) results between certain V-alloy systems below 5.6 e/at. is not to be attributed to band rigidity in a strict local sense, but only in a "soft" average sense where local differences are masked in bulk measurements over ranges where the Fermi density of states varies linearly with all local electron concentrations.

At concentrations past 5.6 e/at., the temperature dependence of the magnetic susceptibility in V-Mn, as in V-Fe below 28% Fe, far exceeds that of the vanadium NMR Knight shift and linewidth. It may be concluded that, whatever the nature of the magnetic moments present, they are most probably localized near manganese atoms in Mn-rich areas where presumably the Fermi level lies well into the upper $3d$ subband.

In looking for an explanation for the temperature dependence of the susceptibility above 45% Mn, one might carry the band description (employed so far in interpreting other observed aspects of V-Mn) one step further, following the approach of Wang, Evenson, and Schrieffer.[44] In their theory, depending on the magnitude of parameters like the density of states at the Fermi level, the Coulomb interaction U, and the virtual level width Γ, one can move smoothly from a temperature-independent Pauli-like susceptibility ($U/\Gamma \ll 1$) to a Curie-law susceptibility ($U/\Gamma \gg 1$) for itinerant d-band-like electrons.

It would not be surprising to expect these parameters to change in such a way that in the limit of

high Mn concentration (either in a local sense or the average sense) a Curie or Curie-Weiss–like behavior would be obtained. It is not so apparent as to what the detailed temperature dependence should be in the intermediate regime. Considering now the local sense, a critical number of nearest like neighbors might drive $U/\Gamma > 1$. There is some speculation that the bcc phase of pure Mn is magnetic.[45] Alternatively, it is possible that the magnetization of Mn atoms in V-Mn proceeds discretely, purely on the basis of microenvironment. This possibility might be realized if Mn atoms are nonmagnetic unless surrounded by more than a critical number of other Mn, where they have the maximum magnetic moment.[46] We have plotted in Fig. 17 $\Delta\chi/c$ as a measure of the magnetization versus the Mn concentration c. Here $\Delta\chi = \chi_{130} - \chi_{300}$ is the difference between χ at 130 °K and that at 300 °K. Since the temperature dependence of χ does not appear to be describable in simple terms, the quantity $\Delta\chi/c$ can only be said to scale with the magnetization. As can be seen in Fig. 17, the probability $P(n^*)$ that an Mn ion has n or more Mn nearest neighbors in a bcc lattice best fits the $\Delta\chi/c$-versus-c curve for $n = 6$. Here $P(n^*)$ is given by the sum over binomial probabilities

$$P(n^*) = \sum_{Z=n}^{N} \frac{N!}{Z!(N-Z)!} c^Z (1-c)^{N-Z}, \quad N = 8 . \tag{3}$$

IV. KNIGHT SHIFT AND SUSCEPTIBILITY PARTITIONING

A. Introduction

In this section, a partitioning of Knight shifts and magnetic susceptibility into their respective contributions will be proposed over the bcc concentration range in V-Mn. The emphasis of this effort will be on the vanadium shifts, but some speculations about the relative magnitude of the contributions to K(Mn) and their concentration dependences will be made.

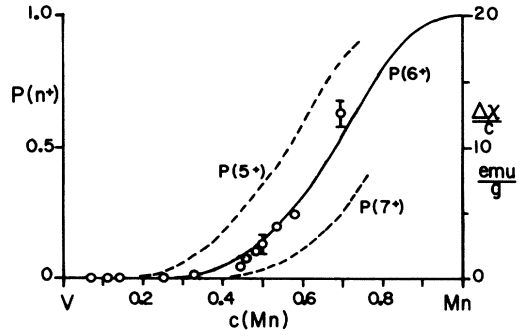

FIG. 17. Probability $P(n^*)$ of n or more Mn being nearest neighbors to a site as a function of Mn concentration. Also shown (circles) is the quantity $\Delta\chi/c$ as defined in the text.

In analyzing the molar magnetic susceptibility χ and the Knight shift K in 3d-band transition metals and alloys, three contributions must be considered in addition to the diamagnetic terms: that of the usual s-conduction electron susceptibility χ_s and the resulting contact hyperfine shift K_s,[47] as well as two contributions arising from the presence of d electrons, the spin paramagnetic susceptibility of the unfilled 3d-conduction band χ_d,[48] and the resulting induced polarization of the s-core electrons, with the associated shift K_d,[49] and last, the Van Vleck orbital susceptibility of the partially filled 3d band χ_0,[50] and the resulting shift K_0.[51] The complete expression for χ_0 given by Kubo and Obata[50] may be approximately represented in terms of an average bandwidth Δ of the 3d subband being filled, and its fractional occupation f[52]:

$$\chi_{obs} = \chi_{dia} + \chi_s + \chi_d + \chi_0 ,$$
$$K_{obs} = K_{dia} + K_s + K_d + K_0 , \tag{4}$$

$$K_s = \tfrac{8}{3}\pi \langle |\Psi_s(0)|^2 \rangle_{E_F} \chi_s/N_0 ,$$
$$\chi_s = \mu_\beta^2 N_s(E_F) N_0 , \tag{5}$$

$$K_d = \tfrac{8}{3}\pi \langle \rho(0) \rangle_d \chi_d/N_0 ,$$
$$\chi_d = \epsilon\, \mu_\beta^2 N_d(E_F) N_0 , \tag{6}$$

$$K_0 = 2\langle r^{-3} \rangle_D \chi_0/N_0 ,$$
$$\chi_0 \approx 4\mu_\beta^2 f(1-f) N_0/\Delta . \tag{7}$$

In these equations, N_0 is Avogadro's number, μ_β is the Bohr magneton, and ϵ is a factor of enhancement of the d-spin susceptibility over the value given by the Bloch free-electron approximation. Butterworth[12] has shown that in V-Cr, $1.0 \le \epsilon \le 1.6$ over the entire concentration range. The expression $\langle |\Psi_s(0)|^2 \rangle_{E_F}$ represents the average at the Fermi surface of the s-electron probability density at the nucleus. The spin density at the nucleus induced by the 3d electrons at the Fermi surface is represented by $\langle \rho(0) \rangle_d$ and is almost certainly negative.[53] Finally, $\langle r^{-3} \rangle_D$ is the average inverse third power of the orbital radius of all 3d electrons.

The diamagnetic susceptibility (core plus conduction electrons) for metallic V was calculated by Butterworth[12] to be

$$\chi_{dia} = -0.15 \times 10^{-4} \text{ emu/mole},$$

and was found to be approximately independent of concentration in V-Cr. The diamagnetic contribution to the vanadium shift may be estimated analogously to the case of platinum,[54] where an approximate but general expression was derived:

$$K_{dia}(\%) = -100\, \Delta n\, r_0/a_0 , \tag{8}$$

where Δn represents the difference in 3d-electron occupancy between the shift reference and the metal, and r_0 and a_0 are the classical electron radius

and the first Bohr radius, respectively. In the case of V metal, the shift is measured with respect to $NaVO_3$, and Δn is about 4. The result is

$$K_{\rm dia}(^{51}\text{V in V metal}) = -0.02\% \ .$$

Because of the relatively small values of $\chi_{\rm dia}$ and $K_{\rm dia}$, any small composition-dependent variations are insignificant and will be disregarded. In the following, χ and K will represent the paramagnetic values, i.e., the observed values minus the calculated diamagnetic contributions.

B. Partitioning for Pure *V* Metal

A partitioning for χ and K in pure metallic vanadium will now be undertaken. The susceptibilities and shifts will be written

$$\chi = \chi_s + \chi_d + \chi_0, \quad \chi = (3.11 \pm 0.02) \times 10^{-4} \text{ emu/mole} ,$$
$$K = A\chi_s + B\chi_d + C\chi_0, \quad K = (0.590 \pm 0.002)\% , \qquad (9)$$

where A, B, and C are the coefficients of the susceptibilities in the shift equations (5)–(7), respectively. The value of B has been deduced by Drain[55] by ascribing all temperature dependence of χ and K to χ_d and K_d, respectively; Mori has shown[56] that χ_0 is nearly temperature independent for vanadium and in V-Cr. Using his own precision measurements of the shift temperature dependence, Drain found

$$B = -(2.0 \pm 0.4) \times 10^{3}\% \text{ mole/emu}.$$

Shimizu *et al.*[57] have calculated the orbital susceptibility for V and V-Cr. For V, they find

$$\chi_0 = 1.78 \times 10^{-4} \text{ emu/mole} .$$

The value of C will now be estimated from Eq. (7);

$$K_0 = (2/N_0)\langle r^{-3}\rangle_D \chi_0, \quad \langle r^{-3}\rangle_{D,\rm metal} = \xi \langle r^{-3}\rangle_{\rm atom} . \qquad (10)$$

With a calculated[51,58] value of $\langle r^{-3}\rangle_{\rm atom} = 2.3$ a.u. and with the assumption $\xi = 0.8$, C is found to be

$$C = 4.1 \times 10^{3}\% \text{ mole/emu}.$$

After the orbital susceptibility is deducted from χ, a fraction x of the remaining spin susceptibility is apportioned to χ_s, leaving the remainder $(1-x)$ $(\chi - \chi_0)$ to χ_d. Interpolating between an upper estimate ($x = 0.2$) given by Shimizu,[57] and a lower limit ($x = 0.08$) found by Cheng *et al.*[6] from electronic specific-heat results for copper, a value of $x = 0.15$ is adopted for V metal, yielding

$$\chi_s = 0.20 \times 10^{-4} \text{ emu/mole}$$

and

$$\chi_d = 1.13 \times 10^{-4} \text{ emu/mole} .$$

Equation (9) is now solved for A to yield

$$A = 4.8 \times 10^{3}\% \text{ mole/emu}.$$

The results of this partitioning are collected in Table II.

These values are in reasonable agreement with those obtained by Butterworth[12] in the V-Cr system, as listed for pure V ($K_s = 0.045\%$, $0.54 \leq K_0 \leq 0.82\%$). Our estimate for χ_s is larger than that of Butterworth's, but the relation between χ_s and K_s is still in approximate agreement with the free-electron model. The orbital Knight shift agrees with the determination by Clogston *et al.*[51] ($\chi_0 = 0.70\%$). A very similar set of values was recently used by Kushida and Murphy,[59] by selecting a consistent set from the most reliable published values. However, when comparing the present results with those of Shimizu *et al.*,[57] it is found that both K_d and K_0 have been overestimated there due to the use of an excessively large value of B.

C. Partioning of *K*(V) in V-Mn

The previous result will now be extended and applied to obtain the concentration-dependent features of the vanadium shift. It is apparent that, while the Knight shift represents the electronic characteristics near the particular nuclei at resonance, the susceptibility samples the magnetic properties of all electrons. In particular, the appearance of population in the upper $3d$ subband is readily apparent from the susceptibility when an increase coupled with a temperature dependence sets in, while the vanadium shift shows an increase in temperature dependence above 45% Mn many times less than that in the susceptibility. It is, therefore, considered necessary, at least in a rough way, to account for differences in electronic magnetic character between regions near solvent atoms and the average, as sampled by susceptibility measurements. In the discussion of the susceptibility, a phenomenological model yielded a measure of an effective charge-density difference $\Delta\rho$ between solute and solvent $3d$-electron orbitals. This model will again be invoked here to derive an effective local susceptibility, so that Knight shift and local susceptibility may be compared and partitioned as functions of the same local electron density. In the case of V-Cr, because of the smaller effective $\Delta\rho$ and the absence of upper $3d$-subband occupancy below 5.95 e/at., considerations of locality are expected to be much less important, and have always been neglected.

Similar features of the electronic band structure

TABLE II. Magnetic susceptibility and Knight shift in V metal, partitioned by contributions.

Origin	$\chi(10^{-4}$emu/mole)	K(V), %	K_i/χ_i, (10^{3}% mole/emu)
s	0.20 ± 0.04	0.096 ± 0.05	4.8 ± 0.4 = A
d	1.13 ± 0.04	−0.23 ± 0.05	−2.0 ± 0.4 = B
o	1.78 ± 0.04	0.72 ± 0.05	4.1 ± 0.4 = C
dia	−0.15 ± 0.03	−0.02 ± 0.005	···
Total	2.96 ± 0.02	0.570 ± 0.003	···

will be assumed to apply to both solvent and solute atoms, with the exception that near solute atoms the band will lie at lower energy so that the increased occupancy up to the Fermi level will result in a $\Delta\rho$ of the magnitude estimated earlier. The previously stated relation [Eq. (2)] between local and average electron density $\bar{e}$ will be used;

$$\bar{e} = (1-c)e_V + c\,e_{Mn}, \quad e_{Mn} - e_V \equiv \Delta\rho \approx 0.3\ e/\text{at.} \qquad (2')$$

Here, c is the fractional Mn concentration. The average susceptibility χ accordingly is now divisible into local contributions χ_b evaluated at local electron concentrations and weighted by the fractional abundance of V and Mn atoms,

$$\chi(\bar{e}) = (1-c)\,\chi_b(e_V) + c\,\chi_b(e_{Mn}) . \qquad (11)$$

This equation is to be solved for $\chi_b(e_V)$, which will be regarded as the local vanadium susceptibility to be partitioned. It must again be emphasized that the assumption of a unique susceptibility function of local charge density for V and Mn is a necessary oversimplification to a complex situation and is most likely to err in the magnetically more complex region above 50% Mn.

Using the relation $\bar{e} = 5 + 2c$, it follows from Eq. (2') that $e_V = 5.0 + 1.7c$ and $e_{Mn} = 5.3 + 1.7c$. Substituting these identities into Eq. (11) reduces the number of independent variables to one. Given the correct starting value $\chi_b(5.0\ e/\text{at.}) = \chi(5.0\ e/\text{at.})$, and the correct initial slope (obtained by trial and error), this equation may be solved numerically using the paramagnetic susceptibilities to obtain values of χ_b.

The values of χ and K(V) were interpolated in increments of 5% Mn from smooth lines drawn through the data taken at 300 °K, and are given in columns 2 and 6 of Table III, while in column 3, χ_b is evaluated at e_V. The results of the partitioning will be discussed in terms of the average concentration c with the understanding that relevant quantities are to be regarded as functions of local electron concentration.

TABLE III. Partitioning of vanadium susceptibility and Knight shift versus Mn content.

c	$\chi_{para}(c)$	$\chi_b(e_V)$	$\chi_d(e_V)$	$\chi_o(e_V)$	K_{para}	K_d	K_o
(%Mn)		(10^{-1}emu/mole)				(%)	
0	3.11	3.11	1.13	1.78	0.390	−0.226	0.720
5	2.98	3.00	1.03	1.77	0.605	−0.206	0.716
10	2.88	2.89	0.94	1.75	0.619	−0.188	0.708
15	2.80	2.77	0.83	1.74	0.633	−0.166	0.704
20	2.72	2.66	0.73	1.73	0.646	−0.146	0.700
25	2.62	2.77	0.80	1.77	0.657	−0.160	0.716
30	2.54	2.88	0.86	1.82	0.660	−0.172	0.736
35	2.45	2.94	0.93	1.81	0.654	−0.186	0.732
40	2.39	2.71	0.78	1.73	0.638	−0.156	0.700
45	2.39	2.02	0.36	1.46	0.612	−0.072	0.591
50	3.18	1.62	0.21	1.21	0.542	−0.042	0.490
55	3.79	1.59	0.32	1.07	0.465	−0.064	0.433
60	4.60	2.67	1.17	1.30	0.390	−0.234	0.526
65	5.37	3.74	2.03	1.51	0.328	−0.406	0.611
70	6.17	5.32	3.10	2.02	0.270	−0.620	0.817

The concentration-dependent partitioning proceeds under several more assumptions. First, because of the supposed flatness and small occupancy of the 4s band, the values of χ_s and K_s will be assumed to have negligible concentration dependences, and the values found for vanadium metal will be used at all concentrations. This assumption is very commonly used throughout the 3d-alloy series, but its validity has recently been questioned, especially in view of the possibility of s-d hybridization.[60] Second, the values of B and C will be assumed constant over the encountered range of local concentrations. The assumption of a constant C is probably subject to little error, since $\langle r^{-3}\rangle_D$ is averaged over all occupied 3d states [Eq. (7)] and will not be changed materially by adding a small fractional occupancy of the upper 3d subband. An expected change in $\langle r^{-3}\rangle_D$ due to alloying, because of its approximate inverse proportionality to atomic volume,[59] is probably small and will be ignored. The assumption of the constancy of B across the change to a different subband is perhaps more debatable, since $\langle\rho(0)\rangle_d$ [Eq. (6)] is averaged only over states near the Fermi level. However, the effects of the upper 3d subband on the partitioned values will be pronounced enough so that a change in B would probably not affect the qualitative features found. The assumption of a constant B would probably lead to more serious error in a partitioning of K(Mn).

If the s-like contributions are deducted from the susceptibility and shift,

$$\chi_{od} \equiv \chi_b(e_V) - \chi_s, \quad K_{od} \equiv K - K_s , \qquad (12)$$

then, using Eq. (9), and solving simultaneously,

$$\chi_0 = \frac{K_{0d} - B\chi_{0d}}{C - B}, \quad K_0 = C\chi_0 ,$$
$$\chi_d = \chi_{0d} - \chi_0, \qquad K_d = B\chi_d . \qquad (13)$$

The results of this partitioning are entered in columns 4 and 5, and 7 and 8 of Table III, and are shown for K(V) in Fig. 18.

As to just how the strongly temperature-dependent susceptibility and the weakly temperature-dependent V shift at high Mn concentrations should be related is not clear. Thus, it is instructive to repeat the partitioning with the refinement of ascribing all the temperature dependence in χ to Mn atoms. This procedure may underestimate the desired V-like local susceptibility at the highest concentrations, whereas the previous approach has probably overestimated it.

In recent completed work on V-Mn[35] the susceptibility in the temperature region above 130 °K has been divided between a temperature-independent term χ_σ and a Curie-Weiss term. For concentra-

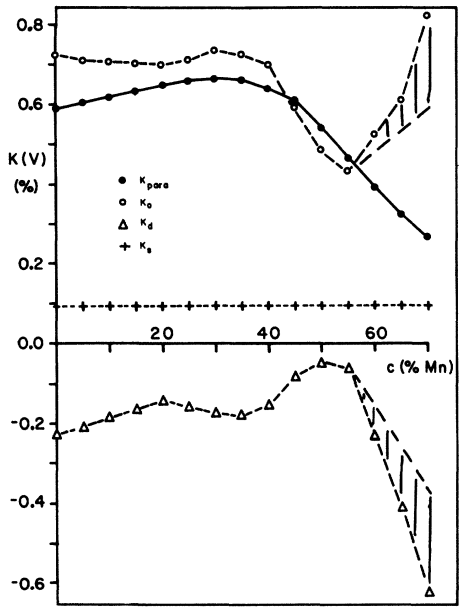

FIG. 18. Results of the partitioning of the room-temperature ^{51}V Knight shift in bcc V-Mn as function of the Mn concentration. The shaded areas for K_0 and K_d denote their possible range from the partitioning of the entire room-temperature susceptibility (symbols) to the inclusion of its temperature-independent part (see text).

tions below about 45% Mn, χ_σ essentially accounts for the entire observed susceptibility, in agreement with our observations, while towards 70% Mn in V, the share of χ_σ in the 300 °K susceptibility falls to near 0.45 of χ_{obs}. The desired alternative partitioning calls for substitution of $\chi_\sigma(c)$[35] for $\chi_{obs}(c)$ above $c = 45\%$ Mn in Eq. (4) and proceeding as before. These results are shown in Fig. 18, where they represent the lower boundaries for K_0 and $|K_d|$. While the features of the partitioned contributions remain similar, the cancellation between K_0 and K_d is less severe in this approach.

Several observations may be made about the results of the concentration-dependent partitioning. The initial increase of the Knight shift is due, as in the case of V-Cr,[12,57] mainly to the decrease in the negative K_d, arising from the well-known decrease in the 3d Fermi density of states. The decrease of K above 35% Mn is caused first by the decrease in K_0, as a result of the closing of the lower 3d subband, again as in V-Cr. There, the entire sizable corresponding decrease in K(V) beyond 5.6 e/at. is due to that in K_0 alone,[12,57] while K_d is only beginning to level off after its decrease in absolute value. In V-Mn, a similar partial cancellation between the changes in K_d and K_0 extends from 35% Mn upward, since both the filling of one subband and the entering of another affect K_0 and K_d in opposite directions [see Eqs. (6) and (7)]. It is, thus, inevitable that the net shift in this region represents the difference between two partially cancelling concentration dependences. It is possible, however, that the suddenness of the derived changes is exaggerated in our model. In V-Mn, the concentration dependence of K_0 may be viewed, in terms of Eq. (7), as arising from a sum of two terms of the kind $f(1-f)/\Delta$, where f is the concentration-dependent occupancy of the first or second 3d subband, and Δ is the width of that subband. The resulting dip in K_0 is, thus, physically reasonable and to be expected in V-Mn, V-Fe, etc., but not in V-Cr, as is found to be the case. It is expected that K_0 would rise to another rounded maximum near 6.8 e/at. if that electron concentration could be reached in the bcc region. The evident (Fig. 18) greater height of that maximum is attributable to the smaller width Δ of the upper subband [Eq. (7)].

The decrease in χ_d and K_d by a factor of 5 between V metal and 45% Mn ($\bar{e} \approx 5.9$ e/at.) is in excellent agreement with the estimate[6] of 3d-state densities from electronic specific-heat measurements in several similar alloy systems, and, recently V-Mn.[35] An approximate spin susceptibility, $\chi_{spin} = N_0 \mu_B^2 N(E_F)$, calculated from the experimental specific-heat density of states for V and V-Mn, is about 10% smaller than the sum $\chi_{sd} = \chi_s + \chi_d(e_V)$ at several corresponding concentrations below 25% Mn. It may be inferred that, except for systematic errors incurred in partitioning, the value of ϵ in Eq. (6) is approximately 1.1 in this region. The concentration dependence of χ_{spin} up to 70% Mn closely follows that of $\chi_{sd}(e_V)$, except for a lag in χ_{sd} attributable to its vanadium locality. The temperature dependence of the V shift in alloys up to 45% Mn in V is equal to, or weaker than, that observed in V metal,[55] consistent with the decreasing χ_d up to 50% Mn. While somewhat greater temperature dependence of K(V) is observed above 55% Mn, the much greater linewidths render the shift measurements less reliable in this region. As expected, in all cases K(V) increases with increasing temperature, confirming the negative sign of the hyperfine field from core polarization at all concentrations.

The similar features of K(V) and K(Mn) invite an analogous partitioning for the latter. Because of the relative lack of theoretical and experimental information on dilute Mn in V, only a qualitative discussion is possible.

The large positive manganese shift in the dilute regime is almost certainly attributable mainly to K_0. The initial approximate constancy of K(Mn) versus c might then be caused by a cancellation of the concentration dependences of $K_d(e_{Mn})$ and K_0 (e_{Mn}). Thus, using the previously obtained χ_d and χ_0, evaluated at e_{Mn}, the concentration dependence of K(Mn) can be satisfactorily reproduced up to 35% Mn using Eq. (9), $C \approx 1 \times 10^4$% mole/emu and

$B \approx -8 \times 10^3$% mole/emu. These values imply not unreasonable estimates of $K_0 \approx 2\%$, $K_d \approx -0.6\%$ in the dilute regime. Between 35 and 70% Mn, the value of B must be gradually increased to more than twice its original size to obtain an adequate fit to K(Mn). Such an increase in B is to be expected as the upper $3d$ subband is populated.

V. CONCLUDING REMARKS

Many physical properties of the bcc V-Mn alloy system, such as Knight shifts and susceptibility, are governed in a large measure by the band structure of the $3d$ band and a strongly concentration-dependent density of states at the Fermi level. The relative smallness of the quadrupole effects in this and other V-based transition alloys is tentatively attributed to an indirect effect which results from the large state density at the Fermi level (see Appendix A).

The applicability of the rigid-band model to V-Mn is only very approximate, and has been generally regarded as unsafe in regions of transition between electronic subbands.[26] It is concluded that a crude correction to the rigid-band model, in the form of a shifting of the electron bands between the average solvent and solute sites, is appropriate in this case. In V-Mn, this shifting, as inferred from comparisons between different V alloys, results in an excess population of the Mn $3d$ shell of about 0.3 electrons over that of the V $3d$ shell. Above 35% Mn in V, the effects of the overlap of the charge clouds arising in shielding the extra solute nuclear charge are becoming evident as microscopic variations in electronic environment for both solute and solvent atomic species. From a consideration of the Knight-shift inhomogeneity, these charge clouds are estimated to have a mean radius of two neighbor shells beyond the charge impurity (see Appendix B).

The paramagnetism of this system (bcc V-Mn) appears to be bandlike in origin. By considering a localized band structure, we find it not unreasonable that most of the band moment can be associated with the Mn atoms at high concentrations of Mn. In fact, below 35% Mn, the results of this study are consistent with invoking only the simple temperature-independent form of band paramagnetism, i.e., a Pauli paramagnetism. The effect of presumably small localized regions of the alloy (involving only a few percent or less of the Mn atoms) is quite pronounced in the susceptibility measurements at low temperature, but this effect can be partially isolated by making a ferromagnetic correction in the form of an infinite-field extrapolation. The V^{51} and Mn^{55} NMR is, by comparison, nearly unaffected, consistent with the concept of confining the apparent ferromagnetic-like behavior to small localized regions or aggregations containing Mn in some form. This form is presumably some intermetallic compound or a ferromagnetic phase of Mn or a Mn-V alloy which may exist only in the presence of the bcc V-Mn phase.

Further work is needed to clarify the discrepancy between the observation of ferromagnetic ordering ($T_C = 106\,^\circ$K) in the σ phase by Nevitt and Beck[61] and the present results indicating the absence of bulk-magnetic ordering above 1.4 °K in three σ-Mn-V samples.

ACKNOWLEDGMENTS

The authors are greatly indebted to Dr. J. Darby for performing the levitation melting on about 25 of the samples, as well as for supplying several existing alloys for this study. Dr. J. Oberteuffer graciously supplied a quantity of very pure vapor-distilled manganese during the latter stages of this study. We wish to thank Professor M. Fine for the use of his induction magnetometer and Dr. D. Bardos for the use of his low-temperature susceptibility facility at Argonne National Laboratory in making some of the susceptibility measurements. We are grateful to Professor P. A. Beck, Dr. H. Claus, and P. Panigraphy for communicating some results and interpretations of work on the V-Mn system prior to publication and for supplying a high-concentration alloy sample. We thank Dr. D. Lam for communicating the results of low-temperature susceptibility measurements on a CsCl-ordered V-Mn sample. We gratefully acknowledge Professor J. T. Waber's permission to reproduce some results of his band calculations for the V-Mn system. Finally, we wish to thank Professor M. Bailyn, Professor A. J. Freeman, Dr. D. Koelling, Professor L. Welsh, and Professor T. J. Rowland for their most helpful suggestions.

APPENDIX A: QUADRUPOLAR EFFECTS IN THE ^{51}V NMR SPECTRUM

^{51}V NMR intensity and line-shape measurements in V-rich alloys were undertaken in order to characterize the expected quadrupolar distortion. The differential resonance spectra were accumulated in the memory of the signal averaging computer at fixed values of rf frequency, rf field strength, H_1, modulation amplitude, and temperature, for a series of samples. The spectral parameters were corrected for small sensitivity changes of the oscillator, and normalized for the number of storing sweeps and for the fraction of vanadium contained within the rf coil. In the following, intensity will be expressed as normalized to the number of V atoms present.

The integrated V line shape is independent of temperature for concentrations below 35% Mn; it appears to be Gaussian only within 0.8 times the full derivative peak-to-peak width, ΔH($\Delta H = 12.4$

±0.2 Oe at 12 kOe) on either side of the centroid. At greater distances, a broader base is observed. For pure V, least-squares fits of the spectrum with two Gaussian lines with identical centroids gave a ratio of widths of about 2 to 1 and a ratio of areas of about 1 to 5. Fits with one and two Lorentzian lines failed to reproduce the shape of the base and the region near the centroid.

If one defines a quantity $A = \Delta H^2 h_1$, where h_1 is the peak-to-peak height of the differential spectrum, the integrated area under a Gaussian line is given by $0.52A$, under a Lorentzian line by $1.81A$. By comparing the integrated area (or that from a fit) for the pure V line with the corresponding value of A, it is found that its total intensity is given by $(1.20 \pm 0.05)A$. The departure from the Gaussian norm is caused by the presence of the somewhat broader wing. Consequently, the normalized intensity of the central portion of the resonance was defined as $I_0 = 1.20A$. The usefulness of this definition in the alloys depends on the observation that the differential line shape within $\pm 0.7\Delta H$ of the centroid remains invariant with addition of Mn up to 35%. The method is only tentatively continued into regions of higher concentration, where broadening and asymmetry are observed.

Figure 19 illustrates how, with addition of Mn, a portion of the resonance intensity moves away from the centroid, but remains within $\pm 10\Delta H$ of it. Except for the small decrease in the dipolar width contribution as Mn is added, ΔH is quite unaffected during this symmetric shape change. Double integration of the differential line confirms the presence of essentially all the intensity within a 250-kHz range. With addition of Mn, the signal-to-noise ratio in the broad wings of the spectrum becomes less favorable as more of the intensity spreads outward and covers a wider range, and as less V is available for resonance, so that the integrated total intensity quickly becomes less precise than the central intensity. The latter decreases at first and approaches 0.2 with addition of Mn for several series of samples, as shown in Fig. 20. This observation indicates that the distortion is of quadrupolar origin.

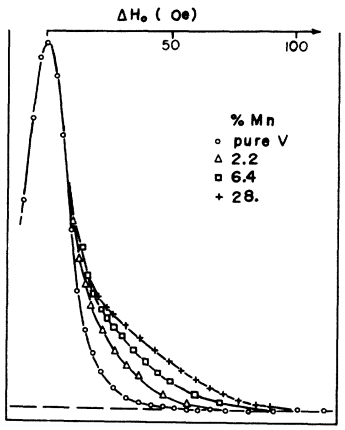

FIG. 19. Integrated ^{51}V NMR lines in pure V and three V-Mn alloys showing first-order quadrupolar distortion. These spectra were taken at 300 °K near 11.9 kOe, and have been normalized to coincide at the centroids. Only the up-field wings are shown. Scale at top is in oersteds. Definition of symbols: open circle, pure V metal; triangle, 2.2% Mn; square, 6.4% Mn; plus, 28% Mn.

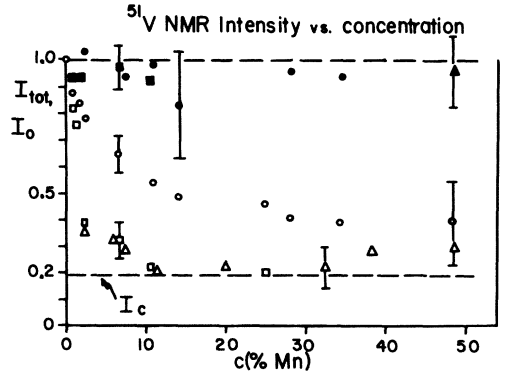

FIG. 20. ^{51}V NMR intensities as function of Mn content at 300 °K near 11.9 kOe. Full symbols denote total intensity ratio I_{tot} between alloy and V metal; open symbols are ratios of central intensity I_0 (for definition, see text). Circles refer to arcmelted and levitation-melted samples; squares refer to the heat-treated sections of these same samples, while triangles denote two series of arcmelted samples.

For ^{51}V, $I = \frac{7}{2}$. The fractional intensity I_c of the central $(m = \frac{1}{2} \leftrightarrow m = -\frac{1}{2})$ transition is $\frac{4}{21} = 0.1904$. Broadening and disappearance of the central transition is describable by second-order perturbation theory,[62] which predicts a line distortion and broadening having a characteristic dependence on inverse applied field. Since no such field dependence was observed within ±0.2 Oe above 5 kOe in any instance, and since the experimental central intensity I_0 asymptotically approaches the quadrupolar central fraction, I_c for most series of samples, we conclude that the observed distortion is describable entirely in terms of first-order quadrupolar effects.[63] In a polycrystalline disordered alloy, the satellite spectra (transitions other than $m = +\frac{1}{2} \leftrightarrow m = -\frac{1}{2}$) are spread over a range of frequencies. Bloembergen has given expressions for setting a lower limit on the electric field gradient q in the absence of satellite intensity near the central resonance, and providing an upper limit for the case of the absence of broadening of dispersal of the central resonance[64]:

$$\langle q \rangle \gtrsim 4I(2I-1)h\Delta\nu/3e^2Q\ ,$$

$$\langle q \rangle < \frac{h}{e^2Q}\left[\nu_0 \Delta\nu \frac{128I^2(2I-1)}{25(2I+3)}\right]^{1/2} \qquad \text{(A1)}$$

Here, $\Delta\nu$ is the experimental resonance width in frequency units. In this case, $\langle q\rangle$ is descriptive of the statistically significant range of field gradients at V nuclei in alloys from 15 to 35% Mn. Using Eq. (A1) with $Q = 0.20$ b, [65] it is found that

$$5.5\times10^{22}\ \text{cm}^{-3} \lesssim \langle q\rangle < 2.6\times10^{23}\ \text{cm}^{-3}\ .$$

The upper limit is calculated at 5 kOe in order to give its lowest value consistent with observation from the appearance of the line it is inferred that the estimated upper limit is reached only at V nuclei having one or more Mn nearest neighbors. This value is among the smallest reported for any alloy system.

Next, the initial rate of decrease in I_0 will be used as a measure of the effective disturbance radius of Mn impurities in the V lattice. The all-or-nothing model, due to Bloembergen and Rowland, [66] will be employed. The following discussion is intended to apply to the series of samples for which the experimental I_0 approaches the quadrupolar I_c at higher concentrations (squares and triangles in Figs. 20 and 21). The series of samples departing notably from this behavior differ from the three other series by an aspect of preparation and will be discussed separately. The all-or-nothing wipeout model, for first-order quadrupolar distortion, results in a relation between the observed central intensity I_0 and the quadrupolar central fraction I_c [66]:

$$I_0 = I_c + (1 - I_c)(1 - c)^n\ , \qquad \text{(A2)}$$

where c is the fractional Mn concentration, and n, the first wipeout number, is the number of host atoms surrounding an isolated impurity whose spectra have the quadrupolar satellites removed from the central region. The experimental value of n for ^{51}V is the negative slope in a plot of $\ln[(I_0 - 0.19)/0.81]$ versus c (see Fig. 21). It is found that $n_{\text{expt}} = 36 \pm 6$, implying that the presence of one Mn atom within three nearest-neighbor shells (26 atoms) of a V atom suffices to remove its satellite intensity; it is likely that the presence of two or more Mn in the fourth shell from a V causes wipeout as well. The measured n is among the smallest reported.

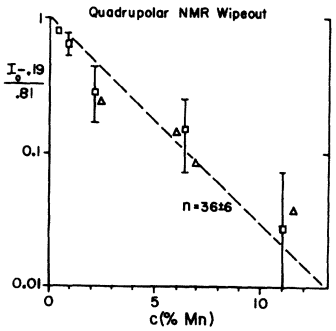

FIG. 21. Experimental fraction of the satellite intensity contained in the central ^{51}V resonance-versus-Mn content for the heat treated or only arcmelted samples. Symbols are the same as in Fig. 4. The value n is the experimental first-order quadrupolar wipeout number.

Of the series of samples used, only the series showing no close approach to I_c at higher Mn concentration were levitation melted without further heat treatment, i.e., they were rapidly quenched by dropcasting from full liquidity. Part of each of these ingots was accorded heat treatment and displayed the complete wipeout behavior. The deviant behavior was apparently caused by the rapid quenching, which, contrary to expectation, seems to have reduced the size or incidence of the field gradients. A tentative explanation of this reduction is the presence of segregation in the liquid phase, partially frozen into the solid solution by rapid quenching. In this case, a tentatively deduced[1] wipeout number of $n = 7 \pm 1$ for this series must be reinterpreted in terms of a significant departure from randomness in the solute distribution. Linewidths and Knight shifts in these samples agreed with values in the correspondingly slowly cooled samples.

As expected from previous work in V-based alloys, [13] the coldworking from filing or grinding did not seem to produce stress sufficient to cause field gradients resulting in broadening or wipeout effects, and no effect of powder annealing was observe on the line shape of pure V. Stress annealing of the powdered alloys was, therefore, omitted to avoid sample contamination.

Quadrupolar wipeout effects have been successfully analyzed in nontransition-metal hosts by a consideration of local charge conservation via the Friedel sum rule, [67] to describe conduction electron scattering and charge-density oscillations surrounding the impurity. For first-row transition solutes, because of the presence of partially filled $3d$ states, the scattering is largely resonant ($l = 2$) and the amplitude of the charge-density oscillations is many times larger than for nontransition solutes. A wipeout number for Cu in Al was found to be about 160, while the same measure for Mn in Al was 850, [68] in good agreement with theory. In transition-metal hosts with a high Fermi density of states $n(E_F)$, another significant contribution to the effective field gradient has been described. [69] It arises from the local repopulation of the conduction electron states near the Fermi surface in response to the lattice field gradient q_{latt} (which includes the effect of charge-density oscillations). This contribution is directly proportional to both $n(E_F)$ and q_{latt}, but is typically opposite in sign to q_{latt}, resulting in "overshielding." We believe that the small values of the field gradients at both nuclear sites in V-Mn, and possibly other V-based alloys, is the result of a partial cancellation between this induced negative contribution and the positive direct contribution of q_{latt} which is amplified by antishielding.

APPENDIX B: EFFECT OF KNIGHT-SHIFT INHOMOGENEITY ON LINE SHAPE

In disordered alloys, shift variations may arise from microscopic concentration variations due to the random solute distribution. Similar, smaller effects are expected as a result of the anisotropic Knight shift because of the resulting departure from cubic symmetry. Among V-based alloy systems, line distortions attributable to these causes have previously been observed in V-Cr[14] and V-Fe.[7] The observation of a temperature-independent field dependence of the linewidth in disordered alloys, coupled with pronounced concentration dependence of the bulk Knight shift, are evidence of Knight-shift inhomogeneity. The most pronounced asymmetry and large field-dependent broadening in the ^{51}V NMR in V-Mn occurs near 50%, the concentration of maximum disorder. A simple model will be used to simulate the vanadium line shape of a 50% disordered alloy; a comparison with the observed spectrum will test this origin of the observed line-shape effects.

The line shape is represented as a sum of contributions, each from a configuration with a different local manganese concentration c'. The latter is defined by the number n' of Mn atoms within several shells of the observed site; the choice of two neighbor shells gave the best preliminary results, so that $c' = \frac{1}{14} n'$. Each of these contributions is to be given the appropriate line shape and width, shift, and intensity. The latter is given by the binomial probability

$$P_N(n, c) = \frac{N!}{n!\,(N-n)!}\, c^n (1-c)^{N-n}, \tag{B1}$$

with $N = 14$. At $c = 50\%$, configurations from $n = 4$ to $n = 10$ account for 94% of the total, so that the rest may be ignored for practical reasons. Each of the seven significant contributions was given the appropriate full quadrupolar distortion by being represented by the sum of two Gaussian lines with equal centroids and having ratios of width and intensity as found from a curve fit of a spectrum of a 28% alloy. The central linewidth was taken as the dipolar width modified by powder demagnetization broadening,[41] and was held constant at 10.5 Oe for all configurations. The shift for each line was estimated from the measured modal bulk shift $K(c)$ by interpolating K for each value of n' at the concentration $c' = \frac{1}{14} n'$, where that configuration is most likely and most closely determines the bulk shift. The comparison of the synthesis with the experimental spectrum was performed by a least-squares curve-fitting computer program which also first integrated the observed differential spectrum. The program was instructed to fit the observed spectrum with the synthesis, which is of the form

$$g_{\text{obs}}(H) = A \sum_{i=1}^{7} g(H - H_i) f_i\,, \tag{B2}$$

where

$$H_i = B - 0.01 H_0 K(n_i/14), \quad n_i = 4, \ldots, 10$$

$$f_i = P_{14}(n_i, c = 0.5)$$

and

$$g(H) = 1.8\, G(H;\ \Delta H = 10.5 \text{ Oe}) + 1.0\, G(H;\ \Delta H = 46 \pm 3 \text{ Oe})\,,$$

where G represents a Gaussian line shape having width ΔH between slope extrema. In the two-parameter fit, only the height (A) and the position (B) of the over-all spectrum were free to adjust optimally. The resulting Calcomp plot is reproduced in Fig. 22, where the integrated experimental spectrum is represented by crosses.

The general peak shape and width, and the direction and magnitude of the asymmetry, are reproduced by the model. The source of the asymmetry is the curvature in the relation $K(c)$ versus c, which nearly superimposes several components at the low-field (left) side of the spectrum, while spreading the high-field components over a wider region. In the absence of curvature, this model predicts only symmetric broadening as found below 30% Mn and approached well above 50% Mn. The imperfect fit in the spectral wings may be caused partly by the neglect of the weak components, i.e., those for which $n' \leq 3$ and $n' \geq 11$ or by the anisotropic Knight shift.

An identical analysis was performed for the much wider Mn spectrum in the same sample. While the model again correctly reproduces the observed width and asymmetry, the very large slope of K(Mn) versus c above 40% Mn separates adjacent configurational contributions far enough to make them individually recognizable in the synthesis. A preliminary calculation shows that applying this model

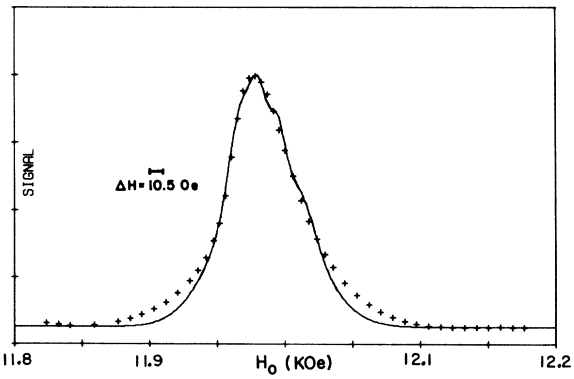

FIG. 22. Vanadium NMR line shape in a disordered sample containing 50% in V. The pluses represent the integrated experimental spectrum. Details of the synthesis (solid line) are described in the text.

with a radius including three shells would produce a smoother synthetic spectrum, but would fail to account for the entire observed width. A more correct approach would replace the sharp cutoff radius with a decreasing weighting of contributions from neighbor shells past the first. The results obtained generally confirm the estimate of shift sensitivity as extending to two neighbor shells. This radius is of the order of an inverse Fermi wave vector and, thus, physically reasonable.

APPENDIX C: ANALYSIS OF KNIGHT-SHIFT DATA TO ESTIMATE $\Delta\rho$

In order to better illustrate our estimate of an excess local occupancy $\Delta\rho$ of the $3d$ band near the solute from the initial Knight-shift slope data in Fig. 11 we proceed as follows: We assume that for small concentrations c of solute the concentration dependence of the Knight shift K given by Eqs. (4)–(7) and (9) arises only from the core-polarization term and χ_s and χ_0 are essentially constant for small c. Furthermore, we assume for small c, that the density of states at the Fermi level is linearly decreasing with increasing electron occupancy. We, therefore, write

$$N_d(\epsilon_F) = D_1 - D_2(\mathfrak{z}' - 5) , \tag{C1}$$

where D_1 is the state density for pure V and $\mathfrak{z}'$ is the local electron per atom ratio for a V site. D_2 is another constant related to how rapidly $N_d(\epsilon_F)$ decreases with increasing Fermi energy and d-band occupation. In terms of the rigid-band or average electron-to-atom ratio, $\mathfrak{z}$, which assumes no excess localization of charge,

$$\frac{\mathfrak{z}'}{\mathfrak{z}} = \frac{5 + c(Z' - 5)}{5 + c(Z - 5)} , \tag{C2}$$

where c is the impurity concentration and Z is the number of solute conduction electrons. For Cr, $Z = 6$, for Mn, $Z = 7$, etc., and $Z' \equiv Z - \Delta\rho$. For small c,

$$\mathfrak{z}' \approx \mathfrak{z}(1 - \tfrac{1}{5} c\,\Delta\rho) . \tag{C3}$$

With

$$K = A\chi_s + B' N_d(\epsilon_F) + C\chi_0 ,$$

where $B' = B\epsilon\mu_B^2 N_0$ and using Eqs. (C1) and (C3) noting that χ_s and χ_0 are essentially constant for small c or $\mathfrak{z}$ near 5, and writing c in terms of $\mathfrak{z}$ and Z, we find

$$\left.\frac{dK}{d\mathfrak{z}}\right|_{\mathfrak{z}=5} = B''(1 - \Delta\rho/Z - 5) , \qquad B'' = B' D_2 > 0 .$$

Since from Fig. 11, $dK/d(\mathfrak{z})|_{\mathfrak{z}=5}$ appears to be linear in Z, and since we want $\Delta\rho \to 0$ as $Z \to 5$, it must be that $\Delta\rho = \alpha(Z - 5)^2$, where α is a constant. Hence,

$$\left.\frac{dK}{d\mathfrak{z}}\right|_{\mathfrak{z}=5} = B''[1 - \alpha(Z - 5)] .$$

Using Fig. 11, we find $\alpha \cong 0.14$ so that $\Delta\rho \cong 0.55$. Note that for $Z < 5$, α must be of opposite sign and that if we use the same magnitude for α we reproduce the observed $dK/d\mathfrak{z}|_{\mathfrak{z}=5}$ for dilute Ti in V as well.

---

*Work supported in part by the National Science Foundation and by the Advanced Research Projects Agency through the Material Research Center at Northwestern University and based on part of the Ph. D. dissertation of Ernst von Meerwall, Northwestern University, 1969.

[1]E. von Meerwall and D. S. Schreiber, Bull. Am. Phys. Soc. 14, 64 (1969).
[2]B. G. Childs, W. E. Gardner, and J. Penfold, Phil. Mag. 5, 1267 (1960).
[3]B. G. Childs, W. E. Gardner, and J. Penfold, Phil. Mag. 4, 1126 (1960).
[4]B. G. Childs, W. E. Gardner, and J. Penfold, Phil. Mag. 10, 419 (1963).
[5]S. Taniguchi, R. S. Tebble, and D. E. G. Williams, Proc. Roy. Soc. (London) 265, 502 (1961).
[6]C. H. Cheng, C. T. Wei, and P. A. Beck, Phys. Rev. 120, 426 (1960).
[7]D. J. Lam, D. O. Van Ostenburg, M. V. Nevitt, and D. W. Pracht, Phys. Rev. 131, 1428 (1963).
[8]R. J. Noer, Proc. Phys. Soc. (London) 84, 599 (1964).
[9]D. O. Van Ostenburg, D. J. Lam, H. D. Trapp, and D. E. McLeod, Phys. Rev. 128, 1550 (1962).
[10]D. J. Lam, J. J. Spokas, and D. O. Van Ostenburg, Phys. Rev. 156, 735 (1967).
[11]R. G. Barnes and T. P. Graham, J. Appl. Phys. 30, 938 (1965).
[12]J. Butterworth, Proc. Phys. Soc. (London) 83, 71 (1964).
[13]L. E. Drain, Bull. Ampere 9, 425 (1960).
[14]L. E. Drain, J. Phys. Radium 23, 745 (1962).
[15]D. O. Van Ostenburg, H. D. Trapp, and D. L. Lam, Phys. Rev. 126, 938 (1962).
[16]D. O. Van Ostenburg, J. J. Spokas, and D. J. Lam, Phys. Rev. 139, A713 (1965).
[17]D. O. Van Ostenburg, C. H. Sowers, and J. J. Spokas, Phys. Letters 20, 461 (1966).
[18]D. O. Van Ostenburg, D. J. Lam, H. D. Trapp, D. W. Pracht, and T. J. Rowland, Phys. Rev. 135, A455 (1964).
[19]D. Zamir, Phys. Rev. 140, A271 (1965).
[20]E. von Meerwall and D. S. Schreiber, Phys. Letters 27A, 574 (1968).
[21]C. H. Cheng, K. P. Gupta, E. C. Van Reuth, and P. A. Beck, Phys. Rev. 126, 2030 (1962).
[22]J. L. Beeby, Phys. Rev. 135, A130 (1964).
[23]J. C. Slater, J. Appl. Phys. 8, 385 (1937).
[24]J. T. Waber (private communication).
[25]E. Vogt and E. Oehler, Z. Physik 176, 351 (1963).
[26]E. A. Stern, Phys. Rev. 157, 544 (1967).
[27]L. Pauling, Phys. Rev. 54, 899 (1938).
[28]R. M. Waterstrat, Trans. Met. Soc. AIME 224, 240 (1962).

[29]J. S. Kasper and R. M. Waterstrat, Acta Cryst. 9, 289 (1956).
[30]J. B. Darby, Trans. Met. Soc. AIME 227, 1460 (1963).
[31]Y. Oda and H. Yamagata, J. Phys. Soc. Japan 25, 629 (1968).
[32]E. von Meerwall and D. S. Schreiber, Phys. Letters 28A, 495 (1969).
[33]These analyses were performed by Schwarzkopf Microanalytical Laborabory, Woodside, N. Y.
[34]W. B. Mims, G. E. Devlin, S. Geschwind, and V. Jaccarino, Phys. Letters 24A, 481 (1967).
[35]P. A. Beck, H. Claus, and P. C. Panigraphy (private communication).
[36]J. H. Van Vleck, Phys. Rev. 74, 1169 (1948).
[37]J. Friedel, J. Phys. Radium 16, 444 (1955).
[38]J. S. Langer and S. H. Vosko, J. Phys. Chem. Solids 12, 196 (1959).
[39]W. Kohn and S. H. Vosko, Phys. Rev. 119, 912 (1960).
[40]T. J. Rowland, Phys. Rev. 125, 459 (1962).
[41]L. E. Drain, Proc. Phys. Soc. (London) 80, 1280 (1962).
[42]L. F. Bates, *Modern Magnetism*, 4th ed. (Cambridge U. P., Cambridge, England, 1960), Chap. III.
[43]E. A. Stern, Physics 1, 255 (1965).
[44]S. Q. Wang, W. E. Evenson, and J. R. Schrieffer, Phys. Rev. Letters 23, 92 (1969).
[45]R. J. Weiss and K. J. Tauer, J. Phys. Chem. Solids 4, 135 (1958).
[46]Previous models of this sort have been successfully applied to magnetic impurities dissolved in binary alloys, where the magnetizing atoms and the magnetic impurities are of different species; cf. V. Jaccarino and L. R. Walker, Phys. Rev. Letters 15, 258 (1965).
[47]C. H. Townes, C. Herring, and W. D. Knight, Phys. Rev. 77, 852 (1950).
[48]M. H. Cohen, D. A. Goodings and V. Heine, Proc. Phys. Soc. (London) A73, 811 (1959).
[49]Y. Yafet and V. Jaccarino, Phys. Rev. 133, A1630 (1964).
[50]R. Kubo and Y. Obata, J. Phys. Soc. Japan 11, 547 (1956).
[51]A. M. Clogston, A. C. Gossard, V. Jaccarino, and Y. Yafet, Phys. Rev. Letters 9, 262 (1962).
[52]D. S. Schreiver, Phys. Rev. 137, A860 (1965).
[53]R. E. Watson and A. J. Freeman, Phys. Rev. 123, 2027 (1961).
[54]A. M. Clogston, V. Jaccarino, and Y. Yafet, Phys. Rev. 134, A650 (1964).
[55]L. E. Drain, Proc. Phys. Soc. (London) 83, 755 (1964).
[56]N. Mori, J. Phys. Soc. Japan 20, 1383 (1965).
[57]M. Shimizu, T. Takahashi, and A. Katsuki, J. Phys. Soc. Japan 18, 1192 (1963).
[58]A. J. Freeman and R. E. Watson, in *Treatise of Magnetism*, edited by H. Suhl and G. T. Rado (Academic, New York, 1965), Vol. IIA.
[59]T. Kushida and J. C. Murphy, Phys. Rev. 178, 433 (1969).
[60]A. J. Freeman (private communication).
[61]M. V. Nevitt and P. A. Beck, Trans. Met. Soc. AIME 203, 669 (1955).
[62]M. Cohen and F. Reif, in *Solid State Physics*, 5th ed., edited by F. Seitz and D. Turnbull (Academic, New York, 1957), p. 321.
[63]R. V. Pound, Phys. Rev. 79, 685 (1950).
[64]N. Bloembergen, *Proceedings of the International Conference on Defects in Crystalline Solids, Bistol, England*, 1954 (The Institute of Physics and the Physical Society, London, 1955), p. 1.
[65]K. Murakawa, J. Phys. Soc. Japan 21, 1466 (1966), has deduced a somewhat smaller value of $Q \approx 0.04$b. If this were used as a lower limit, the upper limit of $\langle q \rangle$ is raised by about a factor of 5.
[66]N. Bloembergen and T. J. Rowland, Acta Met. 1, 731 (1953).
[67]J. Friedel, Can. J. Phys. 34, 1190 (1956).
[68]J. M. Brettell and A. J. Heeger, Phys. Rev. 153, 319 (1967).
[69]R. E. Watson, A. C. Gossard, and Y. Yafet, Phys. Rev. 140, A375 (1965).

PHYSICAL REVIEW B VOLUME 3, NUMBER 1 1 JANUARY 1971

Mössbauer Recoilless Fraction of Solid Krypton. II

J. S. Brown
Department of Physics, University of Vermont, Burlington, Vermont 05401
(Received 27 July 1970)

The Mössbauer recoilless fraction of solid krypton is calculated in the temperature range 0–85 °K, using a simple treatment of the effects of lattice anharmonicity and thermal expansion upon the phonon frequency spectrum. The model calculation is compared to recent experimental and theoretical studies.

I. INTRODUCTION

In a recent paper[1] the present author presented a calculation of the Mössbauer recoilless fraction of solid krypton using a simple treatment of the effects of lattice anharmonicity[2] upon the phonon spectrum. The harmonic phonon spectrum used in I was based upon a sampling of the first Brillouin zone using a simple first-neighbor Born–von Karman force-constant model for the interaction of the atoms in the Kr lattice.[3]

In the present paper we also include the influence of thermal expansion upon the phonon frequencies, an effect which shifts the frequencies in the opposite direction from the anharmonicity correction included in the earlier paper.